UNIVERSIDADE D
COIMBRA

Daniel Silvério Almeida

Respiratory Analysis for Wireless Monitoring of Untethered Patients in Smart Beds

Master's Dissertation in Electrical and Computer Engineering, supervised by Dr. David Bina Siassipour Portugal and Prof. Dr. Mahmoud Tavakoli and presented to the Faculty of Sciences and Technology of the University of Coimbra.

September 2022

FCTUC FACULDADE DE CIÊNCIAS
E TECNOLOGIA
UNIVERSIDADE DE COIMBRA

Respiratory Analysis for Wireless Monitoring of Untethered Patients in Smart Beds

Daniel Silvério Almeida

Coimbra, September 2022

Respiratory Analysis for Wireless Monitoring of Untethered Patients in Smart Beds

Supervisor:

Doctor David Bina Siassipour Portugal

Co-Supervisor:

Prof. Dr. Mahmoud Tavakoli

Jury:

Prof. Dr. Jorge Miguel Sá Silva

Prof. Dr. Mahmoud Tavakoli

Prof. Dr. Teresa Martinez dos Santos Gomes

Dissertation submitted in partial fulfillment for the degree of Master of Science in Electrical and Computer Engineering.

Coimbra, September 2022

Acknowledgements

During the development of this dissertation there were some difficult moments, but also moments of conquest and joy. With these short words, I would like to thank from the bottom of my heart the most important people who made it possible for me to move forward and improve: my family and my friends.

It was only through their care and motivating words that I felt I could achieve something, even in those moments when it seemed as if time would stop and never start again. I want to thank my father and his infinitely wise words, "If it does not work, it's because you did not do it right." To which I always reply, "Really!!! I never noticed that before, thank you" but that has always been there for me as well. I would also like to thank my mother, who is always willing to help me where she can, and my grandmother for her endless love and affection. I would also like to thank my godmother, uncle and cousin for always keeping me in their hearts.

I would also like to thank my friends for their interest and their silly sense of humor that makes you feel that life is worth living, where a simple late night gathering can turn into a low-light drinking jam party until morning, or a silly conversation on the stairs of Deec after a walk to nowhere but the present. I also want to thank Oda for the wonderful world of joy that is One Piece, which makes you feel like a kid again and reminds you that life is a treasure.

As for my work, I would also like to thank Professor David for his guidance, which has proven to be a valuable help in getting on the tracks that I sometimes forget to follow. I would also like to thank Micael Couceiro for his suggestions on some problems I had when implementing some algorithms. I would also like to thank José Faria for his help in setting up the equipment I used, as well as Professor Mahmoud and his team for their time, contribution and willingness to help me test the hardware, and finally I would like to thank Gonçalo S. Martins for taking the time to review my work and convince me to read Style: The Basics of Clarity and Grace, which I hate to admit was one of the best books I have ever read.

Resumo

Tudo o que queremos alcançar, cada experiência que desejamos vivenciar e qualquer esperança de uma vida boa pressupõe, em primeiro lugar, uma boa saúde.

Não é por isso surpreendente que muitos esforços e recursos sejam investidos na melhoria da qualidade da assistência à saúde, seja por meio de estudos do corpo e da mente ou pela aplicação de novas tecnologias. Felizmente, a maioria dos sintomas que afetam a nossa saúde são representados em fenómenos fisicos, e podem portanto ser medidos. É por esta razão que cientistas de todo o mundo se esforçam para desenvolver métodos versáteis, compactos, energicamente eficientes e de baixo custo, não só para a deteção destes sinais, mas também para a extração relevente dos mesmos.

Essa aplicação de sensores levou ao surgimento de redes de sensores corporais que continuamente monitorizam os sinais mais relevantes para a condição fisica de um paciente ao anexar sensores diretamente ao seu corpo. Isto é feito não só para verificar a condição do paciente, mas também com a esperança de poder detectar mais cedo sinais de condições de saúde graves. Um dos exemplos desse tipo de arquitetura é o projeto WoW, que visa utilizar sensores mais confortaveis para os pacientes e extrair deles informações significativas. Assim, o principal objetivo desta dissertação é implementar formas de monitorizar a respiração de um paciente de forma fiável, visto que este sinal é um dos mais importantes em qualquer aplicação de saúde. Esta dissertação implementa 2 métodos para a monitorização da respiração dos pacientes. Para isto, é proposto um algoritmo para calcular a taxa de respiração em tempo real. No entanto, em situações de alto ruído, como por exemplo, quando um indivíduo está a andar, o método mostrou possuir algum erro.

Algoritmos de extração *ECG Derived Respiration* (EDR) foram também implementados para fornecer uma fonte secundária de respiração e melhorar a qualidade da taxa de respiração extraída. Esses métodos de EDR foram testados com dados recolhidos com o hardware local assim como em *datasets* amplamente usados. Onde os resultados dos testes realizados demonstraram que estes médos são capazes de extrair ondas muito semelhantes ao sinal de respiração original, e o seu desempenho é equivalente ou melhor que os demais métodos de última geração testados.

Abstract

Everything we want to achieve, everything we want to experience, and the hope for a good life, assumes first of all good health.

Therefore, it is not surprising that many resources are being put into improving the quality of healthcare, whether through studies of the mind and body or through the application of new technologies. Fortunately, most of the symptoms that affect our health manifest in physical ways and can therefore be measured. As a result, scientists around the world are striving to develop low-cost, compact, energy-efficient, and versatile methods to not only detect these signals, but also extract reliable information from them.

This application of sensors has led to the emergence of body sensor networks that continuously monitor relevant signals by attaching sensors directly to a patient's body. This is done not only to check on the patient's condition, but also in the hope of early detecting signals of more serious health conditions. An example of this type of architecture is the WoW project, which aims to use sensors that are more comfortable for the patient while still providing meaningful information. Therefore, the main goal of this dissertation is to find ways to reliably monitor a patient's breathing, as this is one of the most important signals in any healthcare application. To this end, this dissertation proposes two methods for monitoring patients' breathing. For this purpose, an algorithm for computing the respiration rate in real time is proposed. However, in situations with high noise, e.g., when a person is walking, this method proved to be erroneous in some cases.

Additional EDR extraction algorithms were also implemented to provide a secondary source of respiration and improve the quality of the extracted respiration rate. These EDR methods were tested with both local hardware data and widely distributed databases. These methods have been shown to be capable of extracting waves very similar to the original respiration signal, and their performance is equivalent or better than the other state-of-the-art methods tested.

"A preguiça é a mãe do progresso. Se o homem não tivesse preguiça de caminhar, não teria inventado a roda."

— Mário Quintana

Contents

List of Acronyms

AI	Artificial Intelligence
ANN	Artificial Neural Network
BLE	Bluetooth Low Energy
BSN	Body Sensor Network
BP	Blood Pressure
BPM	Breaths Per Minute
CBR	Case-Based Reasoning
CNN	Convolutional Neural Network
DTW	Dynamic Time Warping
ECG	Electrocardiogram
EDR	ECG-Derived Respiration
EIP	Electrical Impedance Plethysmography
EMD	Empirical Mode Decomposition
EMG	Electromyogram
FFT	Fast Fourier Transform
FN	False Negative
FP	False Positive
GPS	Global Positioning System
GSR	Galvanic Skin Response

HAR	Human Activity Recognition
HLIF	High Level Information Fusion
HMM	Hidden Markov Model
HRV	Heart Rate Variability
IMF	Intrinsic Mode Function
IMU	Inertial Measurement Unit
IoT	Internet of Things
JDL	Joint Directors of Laboratories
KF	Kalman Filter
K-NN	K-Nearest Neighbors
LLIF	Low Level Information Fusion
LSTM	Long Short-Term Memory
MAS	Multi-Agent Systems
MEMS	Microelectromechanical systems
ML	Machine Learning
OSA	Obstructive Sleep Apnea
PC	Principal Component
PCNN	Pulse Coupled Neural Network
PPG	Photoplethysmographic
RBS	Rule-Based Systems
RIP	Respiratory Inductance Plethysmography
RNN	Recurrent Neural Network
RPM	Respiration Per Minute
RPS	Rotations Per Second
SVD	Singular Value Decomposition

SVM	Support Vector Machine
TN	True Negative
TP	True Positive
UAV	Unmanned Aerial Vehicle
VSM	Virtual Sensor Manager
VSN	Virtual Sensor Network
WoW	Wireless biOmonitoring stickers and smart bed architecture: toWards Untethered Patients
WPT	Wireless Power Transfer
WSN	Wireless Sensor Network

List of Figures

List of Tables

1 Introduction

1.1 Motivation

Healthcare is one of the topics that people put more resources and energy into. Over the years, in the search for ways to improve our current level of treatments, several seemingly unrelated technologies have been applied to healthcare, from automatic fall detection to emotion recognition, in efficient, energy-conscious ways [18, 43, 48]. Today, we strive for solutions that are cost-effective, compact, energy-efficient, versatile, and multicommunicative to detect and monitor various health conditions.

In many cases, the most important and powerful tool that we have at our disposal to prevent major problems is the early diagnosis of potential risk signs that can develop, if untreated, into a stage where a patient can no longer be helped. Looking for these risk signs in otherwise healthy-looking patients, and to accurately and quickly react to changes in the conditions of those who are already in treatment is a major challenge.

This difficulty in monitoring the condition of patients stems from the fact that health professionals are typically only a few when compared to the number of patients under their responsibility. Since they have several other responsibilities, full on medical monitoring is out of the question. Therefor in order to alleviate the need of constant human intervention, various technologies have been developed for this end.

1.2 Sensors in Healthcare

Fortunately, a wide range of problems can be diagnosed using physical means [25] measured using sensors such as thermal sensors, airflow sensors, accelerometers, gyroscopes, pressure sensors, magnetometers, light sensors, and so on. Unfortunately, the most common methods for patient monitoring make use of very large, expensive, battery-dependent, and uncomfortable devices. Yet thanks to new and remarkable advances in Microelectromechanical systems (MEMS) technology, new flexible, skin adherent, wireless powered sensors are being developed to measure signals from the patient body in a less intrusive and uncomfortable

way. This new technology not only improves the overall quality of the monitoring process for patients, but it also improves the reading quality by allowing the placement of dedicated sensors in previously impractical areas due to the nature of traditional sensors. It also provides the ability to obtain data on the same phenomenon from different parts of the body and improve confidence in the physical values measure and to estimate more complex representations about the patient, such as using posture, oxygen and blood pressure data to determine whether the patient is walking or sitting.

Although getting more and more accurate data while increasing patient comfort in using the sensors is not enough to truly improve healthcare conditions, processing, organizing, and classifying that data is necessary to track what the symptoms mean for the patient's current condition to get meaningful results.

To solve this problem in an automated manner, numeral algorithms are being explored to extract meaningful information from the collected data. In this way, robust, accurate signal processing algorithms can be used both in hospitals and in monitoring patients at home, with the goal of eliminating the need for constant human monitoring. This not only helps reduce the burden on patients, but also frees up healthcare staff and resources without compromising, and sometimes even improving, the quality of patient care. Another advantage of the studies conducted is the discovery that it is possible to retrieve the same information from multiple sensor sources. This opens up the possibility of eliminating some of the sensors needed to monitor patients' conditions and replacing them with better, less expensive sensors.

1.3 Context and Outline

An example of a study using multiple wearable sensors to continuously monitor a patient's condition is the WoW project [1] [14], under which this dissertation was developed. The goal of this project is therefore to provide an intuitive system capable of remotely monitoring a patient's relevant physical signals and making simple condition assessments, typically combining individually performed health assessment algorithms into a more general model. The focus is therefore on exploring the reliability of health monitoring using an architecture that includes wearable sensors, IoT modules, and knowledge extraction and data processing algorithms.

To this end, a skin patch was developed in conjunction with wireless communication hardware that adheres so firmly to the skin that it does not come off easily even when the patient is moving or sweating profusely, paving the way for clinical trials. The architecture

[1] https://inovglintt.com/financiamento/wow/

of the project is therefore shown in Fig. 1.1, and the areas that this dissertation mainly focuses on, namely data processing and analysis, are highlighted in orange.

This dissertation adresses the analysis and use of methods for continuous monitoring of a patient's respiratory data, such as classification of the patient's respiratory rate. However, for a more robust analysis of a patient's breathing, various EDR extraction algorithms are also applied to the ECG data. This not only ensures that the patient's breathing can be monitored even if one of the sensors fails, but also allows for a more accurate diagnosis of the patient's breathing. This is critical as it can help monitor the most immediate issues related to the patient's condition, such as the occurrence of hyperventilation.

In addition, the above methods are tested using either a belt with a set of MEMS sensors, including a respiratory sensor, an Electrocardiography (ECG), and other sensors commonly used in healthcare, or a set of widely used databases. This is done not only to compare the performance of the implemented algorithms with other state-of-the-art approaches, but also to evaluate the robustness and adaptability of the implemented algorithms with different datasets and to test their applicability in real-time scenarios.

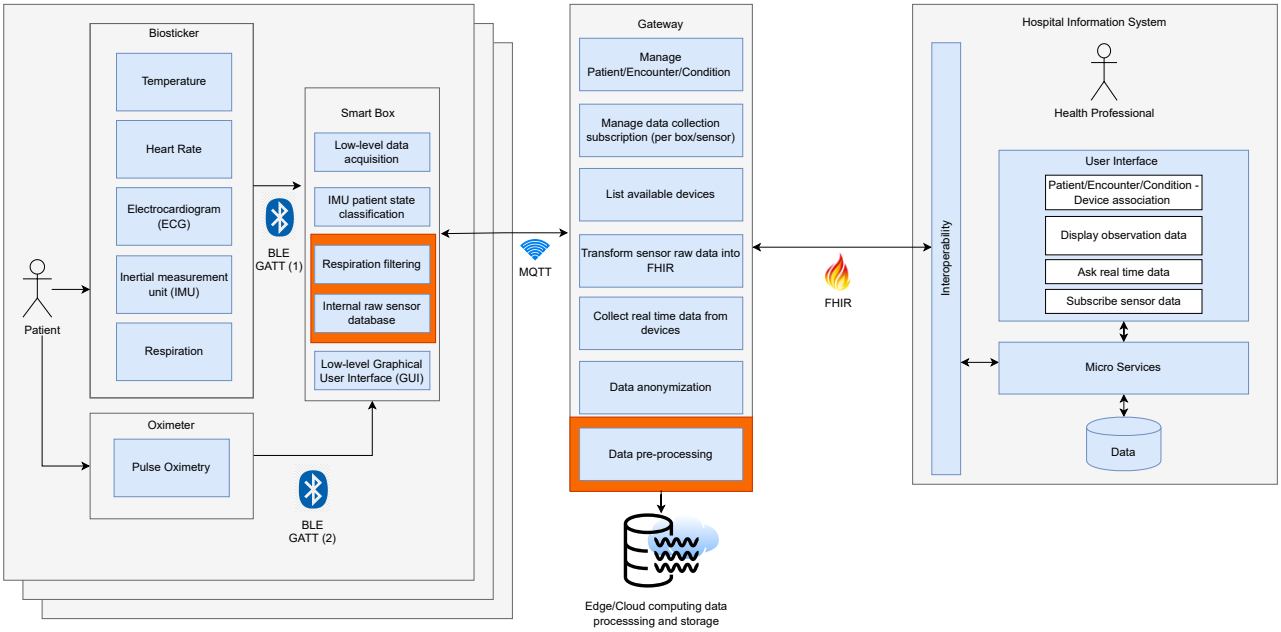

Figure 1.1: WoW project architecture with the areas of focus for this dissertation signalize in orange [1].

The remainder of the dissertation is divided as follows: Section 2 reviews existing work and general techniques for monitoring respiration, addressing the aspects that are most relevant to this work. Section 3 presents the implemented methods in detail and Section 4 examines the results. Finally, a conclusion for this work is presented in Section 5.

2 Related Work

In this chapter, an overview of the studies conducted in the field of respiratory monitoring is presented. The purpose of this review is to familiarize readers with some of the main techniques used in this field, as well as their advantages and disadvantages. However, it should be noted that the sensors used in these works tend to differ. Therefore, a brief introduction to the concept of multi-sensor fusion is given to show how it can be used to improve the current paradigm of health monitoring. To this end, this chapter first explores the sensor context, then builds on this to show the application of multi-sensor fusion, and finally provides an overview of respiratory monitoring methods.

A transducer is a device that converts a change in a physical quantity, such as temperature, flow rate, light intensity, pressure, or other parameters, into an electrical signal [44]. Engineers have been using information from sensors to assess the state of a given physical phenomenon in order to estimate and monitor its condition and make decisions based on our perception of the current state of the world. That is, we attempt to capture the world into a model based on all of its relevant properties in order to monitor and control it in a way that is beneficial to us [44]. In the process, we have developed increasingly precise and dedicated sensors for measuring a wide range of relevant phenomena of interest in a broad range of environments. However, this does not come without a cost, either because the dedicated sensor is too large or bulky and actually influences the medium being measured, there is too information being acquired that the embedded computers cannot keep up with it [25], or because of power consumption [22, 25, 48]. These facts need to be kept in mind when addressing this kind of systems. The bottom line is that sensor-based systems have been subjected to new approaches over the years to mitigate these problems.

Consequently, since there are no universal sensors capable of measuring all physical phenomena, and since real-world systems are complex and subject to a variety of forces, it is impossible to have an accurate understanding of what the world around our systems is without the incorporation of multiple sensors. This leads to the notion of incorporating information from multiple sensorial sources in a model to improve the efficiency of the system, thus performing multi-sensor fusion [25, 44].

2.1 Benefits of Multi-Sensor Fusion and its Application in Healthcare

Multi-sensor fusion is defined as any stage of the integration process in which different sources of sensory information are actually combined into one representational format [44] as can be seen in Fig. 2.1 where multiple sensor data is fused in order to obtain an output of the desired information.

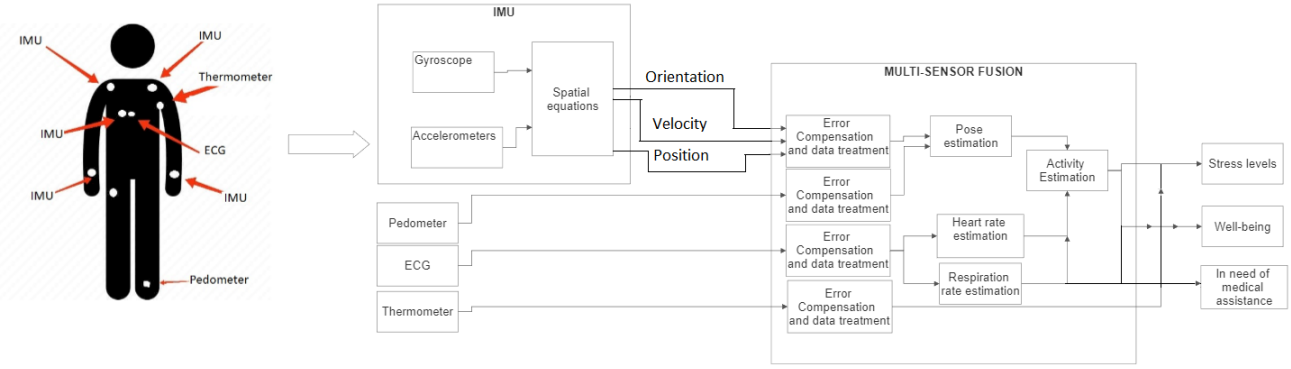

Figure 2.1: An example of using multiple sensors and combining their data to achieve a desired result. In this case, position, thermal, cardiac, and respiratory data are used to assess a patient's stress level, well-being and if they need urgent care.

This definition can be extended by the Joint Directors Laboratories (JDL) definition about information fusion, which defines it as a process dealing with the association, correlation, and combination of data and information from single and multiple sources to achieve defined position and identity estimates, as well as complete assessments of situations and their significance [55].

The multi-sensor fusion process can be done either to provide more complete and reliable information about a physical phenomenon of interest, obtain positional and environmental awareness, select the appropriate set of sensors to better complete the task at hand or to determine if a sensor is faulty [25, 44, 55].

In order to accomplish this, a variety of useful techniques and technologies can be used to build on the advantages that multi-sensor fusion offers when adressing a variety of real world phenomena.

2.1.1 Advantages of multi-sensor fusion

Because multi-sensor systems are used in a wide variety of environments and circumstances, there are numerous potential sources of error, such as the sensor actively interfering with the property being measured, as well as other types of errors. For example, accelerometers, which are one of the most commonly used sensor types for measuring acceleration and classifying position, can be subjected to rotational error, a type of error caused by potential sensor displacement, as well as random noise from uncontrollable sources [75]. This can be extended to virtually all kinds of sensor and multi-sensor architectures, because most models that employ these strategies are subject to the following assumptions [75]: The sensors are placed in an optimal position to detect activities so that they do not interfere with the measured phenomena, and they are also assumed to be stationary over time; To reduce obtrusiveness, the number of sensors is reduced; The sensor's characteristics remain constant over time, which means that it will always measure with the same level of accuracy in the predicted environments; Sensor interconnections are dependable, never failing and always transmitting accurate data.

However, this is not always possible, and problems can arise to undermine these assumptions. Sensors placed in harsh environments eventually degrade and fail [38, 75], and those that use wireless communication or measure any type of wave-based phenomenon are always susceptible to inference and failure [38, 75], just like the unavoidable deterioration caused by the passage of time and the disconnection of sensors and servers, therefore countermeasures need to be put in to place.

As an example, in order to reduce power consumption and space constrictions, MEMS technology is frequently favored over other sensor types, despite its potential for unreliability and fault [15, 75]. When adding jitter to this and other sources of noise and error that are characteristic of all kinds of sensors, such as the material they are made of and the quality of the build and position [68], creates the need to implement solutions that take this into account. For instance a thermometer measuring temperature, may give incorrect readings because the room temperature is significantly different from the one that it was designed to measure in, meaning that if not taken into account it will display different values of relative temperature change [32, 71].

Most of these issues can be avoided, or at least mitigated, by implementing a systems which use multiple sensors to measure the same physical or completely unrelated phenomena [25]. Where some of the most outstanding benefits of multi-sensor fusion systems [25] include: **The noise ratio of the data** to be examined can be **reduced by fusing data from several sensors of the same type** to provide a more accurate depiction of the true value.

Mitigating the effects of malfunctioning sensors, noise, and poor sensor selection;

It can **reduce ambiguity, improve robustness, and confidence in measured data** by fusing sensor data from multiple sources, as it can compensate for faulty sensors, as well as verifying the quality of a sensor by comparing it to the overall value read by consensus; Multi-sensor fusion can also **identify the correct sensors to measure a specific parameter** by comparing the data received and analyzing the course of action that improves its ability to meet the assigned functions [38, 44]; It can **increase the system's robustness against environmental interference** by using different sensors to measure the same phenomenon, which also improves the data resolution; By **placing multiple sensors in different areas of interest**, one can obtain an overall and more **complete estimation** of the target variables, while also **improving precision** [25, 55]; It can provide **coverage of all relevant aspects of a phenomenon** that a single sensor cannot measure, because it is possible to classify complex tasks (e.g running) that involve a complex array of parameters and truly understand it by evaluating different complementary physical aspects, e.g heart beat and acceleration; It **decreases the logic complexity of the systems by allowing for the standardization of inputs**, reducing the logic component to a lower level of the application, making maintenance easier, and making the systems more reliable, effective, and cost-efficient, freeing resources;

Due to the booming revolution of IoT and wireless communication safety protocols, the use of multi-sensor fusion opens the path to **wide area monitoring, either of targets, field conditions, or remote relevant data sources**. It allows the generation of a larger data sets to reduce ambiguity, improve coverage efficiency, ease maintenance and fault detection, and generally providing more relevant data to improve decision making [6, 55]; Multi-sensor fusion allows systems to **respond to unforeseen issues** as it enables the detection of faulty sensors and uses this information to solve the problem. This can be done either by forcing a reinstallation of the sensor software if possible, or by allowing the closest sensors capable of measuring the same phenomena to take over the "workload" of the faulty sensor and trigger a warning so that the faulty sensor can be manually corrected so that the system continues to meet requirements [21]; Multi-sensor fusion enables the **detection of patterns on bigger, more complete data sets**, as well as the detection of potentially lethal circumstances and the discovery of correlations between data to further **reduce the number of sensors while retaining performance** [15, 23, 41];

All of this contributes to the development of more stable, reliable, accurate, precise, and flexible systems, as well as their performance improvement while maintaining an appropriate balance between cost, hardware, computational burden, and the range of the system's capabilities, strengthening the position of multi-sensor technologies in the current world.

2.1.2 Application in Healthcare

Multi-sensor fusion is a technique used to assemble information from multiple sources to improve the understanding and monitoring of complex systems. So it is not surprising that it has found application in the monitoring and knowledge discovery of one of the most complex systems known, the human body. Healthcare professionals use the information collected by different sources to make a diagnoses, and so it is possible to apply data fusion to improve the diagnosis validity, such as in [4], where the usage of structured and unstructured data of relevant cases is used to improve heart diseases monitoring. Multi-sensor fusion can improve the ways we monitor the human body while also improving patient conditions and allowing for continuous monitoring even when the patient is not in a specialized facility [47], usually in the form of an BSN(Body Sensor Network). The benefits of this type of approach are numerous, with the following being some of the most important:

1. With the development of more reliable, smaller, and flexible sensors, it is now possible to **increase the comfort of a patient who requires long-term monitoring**, because new body-worn materials can be used to create multi-sensor wireless systems that move with the body, **not obstructing any major movement while remaining comfortable and fixedly placed above the skin** [3, 25];

2. The ability to use IoT to **remotely monitor a patient signal** enables comfortable home monitoring, **reducing the time required for routine trips, freeing personal and resources of dedicated facilities**, all while assisting the patient in being comfortable and relaxed in their home, **reducing stress** [19, 25, 43];

3. With the use of multiple sensors, it is possible to not only have**more reliable, accurate measurements of key vital signals**, also to use this fused information to **identify patterns**, either between sensors signals or other factors. This allows for the discovery of more **efficient treatments** as well as the possibility of **early detection** of symptoms of diseases that can be then promptly diagnosed and treated [19, 25];

4. **Faster and more accurate** diagnoses and decisions [19].

In this regard, BSNs are very similar to standard wearable multi-sensor systems; however, due to the nature of the topic and the subjects being measured, the sensors must be lighter, smaller, more ergonomic, bio-compatible, with easy battery access and a fast battery charge cycle for the most on-time autonomy possible, as well as more reliable and with stricter safety protocols, either between the sensors themselves and between sensors, and servers [19, 25, 38].

This is only possible through the use of cutting-edge technologies such as IoT (Internet of Things) and ML (Machine Learning). Since a large amount of diverse data can be collected from different patients and used to train models for generic monitoring of daily life or regular checkups, as well as models that look for specific patterns for diagnosis. As such, multi-sensor fusion techniques are used in healthcare today [19, 25], with contributions to healthcare [19, 25]: activity recognition [22]; activity level estimation [47], caloric expending estimation [26], joint angle estimation [41], activity based prompting [20], medication adherence assessment [9], telecare [47], emotional classification [43], disease patterns [61], genome patter recognition [72], rehabilitation [16].

In conclusion, previous works have shown that the use of this technology can be beneficial to healthcare, contributing to its improvement at a lower cost [4].

2.2 Artificial Intelligence

An important factor is the ability to fuse signals and analyze the resulting arrays of data to extract meaning. This can be done trough AI, which can be defined as follows:

> "**Artificial intelligence (AI)** is an integration of computer science and physiology. Artificial in simple language is the computational part of the ability to achieve goals in the world. Intelligence is the ability to think to imagine creating memorizing and understanding, recognizing patterns, making choices adapting to change and learn from experience. Artificial intelligence concerns with making computers behave like humans in a more human like fashion and in much less time than a human takes" [35] .

Having proven to be very useful in the field of healthcare where multiple subsections of AI where adapted in diverse forms for an array of problems like incomplete datasets, image recognition and classification, finding patterns in large datasets [54], searching online for possible drug reactions [60], analysing complex time related variables [28, 27] and even recently in the fight against the COVID-19 [66].

Nevertheless, in the context of healthcare, there is no need for complex implementations when a reliable and summary representation of the available data is sufficient for decision making and monitoring by healthcare experts [4]. Therefore, the general goal of AI applications in healthcare is to generate a less complex, more tangible solution for prediction and classification when possible.

Successful implementations of classical AI Techniques include case-based reasoning [33, 39], rule-based systems [8, 70], fuzzy-based systems [34, 17], and multi-agent systems [74, 77].

2.2.1 Respiration Classification

One major problem regarding the monitoring of patients' health conditions revolves around the idea of appropriately assessing the patient's respiration rate in order to evaluate any potential danger levels deviated from respiratory irregularities. Respiratory Inductance Plethysmography (RIP) can be utilized for automatic breath segmentation in free living situations for numerous patterns of breaths for different activities to provide more comprehensive monitoring [42].

That is, in order to have a proper reading of the respiration rate, especially in wearable sensors, data segmentation is required to extract valid conclusions, whilst being non-intrusive. Which not only makes the patient more comfortable but also reduces the chances of interfering with the medium that is being measured, such as the ventilatory flow. Respiration segmentation techniques are of particular interest because visual analysis of this information from a source other than manual recording is desirable because it is less time consuming and less prone to human error than the current standard of impractical, laborious monitoring by healthcare professionals [42].

Continuous monitoring of a patient respiratory information can help in the early diagnosis of a wide range of respiratory disorders, such as sleep breathing disorder, chronic obstructive pulmonary disease, sudden infant death syndrome and neuromuscular disorders, narcotic medicines, hyperpnea, tachypnea and muscle weakness [11, 53].

A wide array of sensors are used for this, divided into sensors that measure motion, volume, or tissue changes, sensors that measure air flow, and sensors that measure gas changes in the blood stream to evaluate not only if the patient is breathing in or out, but also the level of important gases in the body waveform [30].

Wearable-worn sensors, such as inertial sensors, are therefore useful for developing low-cost and easy-to-use respiratory monitoring systems because they are flexible and small, especially for measuring respiratory rate, and are more convenient for the patient than the very accurate but intrusive carbon dioxide sensors, ECG, transthoratic inductance, and impedance plethysmography [5, 11, 53].In addition, respiratory rate can be calculated automatically, unlike current methods for shorter examinations where medical personnel count the respiratory rate manually. In terms of techniques for determining respiratory rate, there are two broad areas that can be described as follows: Peak detection, a relatively good approach since it is a simple model that detects the peaks of a wave and counts them to calculate the respiratory rate with acceptable results, such as in [42, 53], but which are less reliable than intrusive methods such as carbon dioxide sensors and ECG. The other major methods for determining respiratory rate are based on the use of IMU and ECG and are

generally very reliable. This is because these methods tend to fuse multiple sensor types to calibrate themselves and perform frequency analysis to reduce the source of error that occurs in these types of measurements. However, they are more complex and require special fusion algorithms and are still not as good as intrusive methods [5, 30].

An example where ECG sensors can be used to monitor a patient's respiration arises from the fact that the ECG wave contains information about the respiratory wave. To this end, there are a number of methods that focus on the extraction of respiratory waves from the ECG, with their main focus being the extraction of an ECG Derived Respiration (EDR) wave.

2.2.2 EDR retrieved waves from ECG signals

The use of ECG sensors to calculate respiratory rate is not a new approach, as it is a widely used sensor in medicine that is noninvasive, inexpensive, and supported by the vast majority of medical institutions, which facilitates the integration of algorithms for EDR extraction, because with the introduction of an IoT module to read and store these values, EDR extraction in itself would require only one processing unit to execute the desired algorithm [31, 49]. Combined with the sensor's ability to detect both cardiac and respiratory activity, this makes the ECG an excellent choice for respiratory monitoring support [31]. Where an electrocardiogram (ECG) is defined as a sensor that measures the electrical current generated by the heart muscle (myocardium) during each heartbeat. It consists of at least two electrodes attached to the body and estimates the movement of the heart muscle by determining the voltage difference caused by the current generated between the two electrodes, which are usually located on the chest [12].

However, what makes the ECG interesting for assessing the respiratory status of a patient is the fact that this mechanism is subject to external disturbances such as electromagnetic noise as well as the movements of the body. This is because respiratory motion can change the electrical impedance of the thorax due to changes in lung volume or the position of the cardiac vector with respect to the electrodes. Combined with the fact that breathing tends to increase the heart rate during inspiration and decrease it during expiration, the breathing wave becomes an additive wave in the ECG signal [31]. Because of this aspect of the ECG signal, a variety of methods can be used to extract an EDR by exploiting the inherent relationship between the ECG and the respiratory waves. This results in two important and critical signals being generated by a single sensor. In this regard, it should be noted that although multi-channel ECG-based methods for EDR extraction exist [31], the focus of this dissertation is on methods that use only one ECG or can be adapted for single-channel ECGs, such as [10, 51], as they better fit the materials and proposal of the project in which

this dissertation is involved.

Below is a brief description of some of the most commonly studied methods for extracting EDR waves, as well as some of the methods used in this dissertation:

Band-pass filtering techniques consist in removing all frequencies from the ECG wave that are not in the frequency range of respiration (typically between 0.05 and 0.7 Hz [31]), leaving only the desired signal unchanged, as this filtering removes the unwanted signal components, sometimes using some linear operations [65]. These techniques are generally more efficient than other EDR techniques in noisy environments and have a particularly low error at low breathing frequencies. However, they are very sensitive to the range of frequencies in which they filter the data, and achieve better results if that range is set to a smaller range closer to the breathing frequency. This is because when trying to filter out a wave that contains all of the breathing frequencies, a wider frequency range, such as 0.1-0.8 Hz, is required. This proves that there is no clear frequency range in the literature that can be universally agreed upon, which means that its selection must be carefully weighed for each individual application. This is because the selection of bigger intervals causes other components of the ECG signal and other noisy signals with lower frequencies to fall within the selected frequency range and distort the derived respiratory signal, as has been demonstrated experimentally, while smaller ranges do not take into consideration most of the possible respiration frequencies. [7, 31, 65] are some works that use band-pass filtering.

Wavelet decomposition methods are based on wavelets, a type of fixed-format wave that can be scaled for different frequencies and shifted in time before being used to perform the Discrete Wavelet Transform (DWT). These wavelets are used in EDR extraction to find the signal most similar to a respiratory signal in the ECG and extract these signals in their respective frequency bands. To do this, a DWT is applied to a given signal. In this transformation, the signal is decomposed into a certain number of coefficients that depend on the mother wavelet. This decomposition consists of successive low-pass and high-pass filters that split the analyzed signal into two different components with half of the original information. Since the frequency content of each decomposition is divided by half, the successive cA (low frequency) decomposition gives an ideal bandwidth. Using these coefficients, it is then possible to reconstruct a signal in a particular frequency band that best represents the mother wavelet. With these coefficients, which in the case of DWT are divided by frequency bands that are halved for each new decomposition level, the EDR wave is generated. For this purpose, the inverse DWT function is used to reconstruct a signal in which each coefficient whose associated frequency band is outside the possible breathing

frequency interval is set to zero. The result is the union of all frequencies of the original signal that are closest to the selected wavelet, and if that wavelet is correctly selected, closest to the respiratory waveform. Normally, the decomposition level corresponding to the desired frequencies is either 9 or 10 [56], but it has been found experimentally that it is necessary to investigate other decomposition levels when the sampling rate of the ECG value is very high. This method, although practical, is not suitable for determining the actual shape of the respiratory signal, since the shape of the reconstructed respiratory signal depends strongly on the mother wavelet used, but it tends to increase its performance with increasing respiratory frequencies. Where [7, 56, 62] are some works that use this methodology.

Empirical mode decomposition methods or EMD for short, are methods for decomposing a signal into its constituent IMFs [76]. Where, an Intrinsic Mode Function (IMF) is defined as a signal whose number of extrema (max and min) is equal to or at most one point different from the number of zero crossings, and whose average between the upper and lower envelopes does not differ from zero at any point [45]. This is important because this IMF maps the upper and lower points of a wave with respect to its frequency. This is important in the case of extracting an EDR wave because the inhalation and exhalation of a patient results in a corresponding additive low-frequency signal reflecting this motion. It is possible to extract an EDR by extracting the IMFs that map the highs and lows of these additive low-frequency perturbations. For this purpose, the IMFs are extracted in frequency order, with the highest frequency assigned to the first. After all IMFs are collected in one signal, those that fall within the frequency range of respiration are selected. Since the IMFs for these frequencies represent the waveform of the respiratory motion added to the ECG signal, they are then combined to form the EDR wave [45]. There are variants of this technique, such as Ensemble Empirical Mode Decomposition (EEMD), which solves the problem of mode mixing by combining concepts of noise-assisted data analysis (NADA) with the EMD algorithm, namely the "more heads think better" approach of ensemble techniques to select the most appropriate IMF that reduces noise and increases the performance of the EDR signal [69]. They are extremely dependent on the chosen domain and are subject to noise and sampling errors that can affect the local extrema. However an important difference between EMD techniques and other methods such as wavelet analysis is that the extracted IMFs depend on the waveform of the input signal as they depend on its local extrema. Thus, the EMD decomposition of the signal is data-driven. While methods such as DWT analysis are based on the selection of an appropriate wavelet. Since EMD is inherently data-driven and therefore adaptive, the methods are usually very flexible. Some research that uses EMD as a basis or in general includes [45, 50, 69, 76].

R-peaks analysis methods use information about a person's breathing contained in the QRS complex and can be divided into two main approaches. The first method consists in analyzing the amplitude of R-peaks to exploit the relationship between their amplitude and the displacement of the electrodes caused by the lung movement. The reason for this is that this movement directly changes the impedance of the thorax and the strength of the current measured by the ECG. This leads to higher values of the R peaks in the QRS complex when, depending on the polarization of the ECG, the sensor is closest to the heart, i.e., when the patient exhales, and thus there is a direct relationship between the amplitude of the peaks of the QRS complex and the respiratory motion. The second method is to analyze the distance between the R peaks to take advantage of the fact that the heartbeat tends to increase when a patient inhales and decrease when he exhales. And so, in most cases, higher concentrations of R-peaks near relatively low concentrations can be interpreted as the direct result of a respiratory cycle, i.e., inhalation and exhalation [29]. The R-peak amplitude is less susceptible to muscle artifacts and has high potential for detecting central apnea episodes [29]. The performance of these methods varies depending on variables such as resting position, age, and gender, as all of these factors strongly influence cardiac output, making the link between the heart and breathing less clear. It is also important to note that these methods tend to fail when the ratio of heart rate to respiratory rate is less than 2 [31]. Another disadvantage of all methods based on analysis of the QRS complex on an ECG signal is that they also require accurate QRS and R-peak detection, as incorrect detection leads to performance degradation [31]. This additional step slows down the entire process, and depending on the algorithms used and the processing power of the devices, it has been experimentally found that these methods may be too slow for real-time use, depending on the algorithm used. Some examples of the different approaches are given in [7, 29, 36, 51, 57, 76].

Principal component analysis methods or PCA, construct the EDR signal by analyzing the QRS complex and extrapolating the relationship between it and the respiratory signal, which contains respiratory-dependent features such as the Q and R waves, and then using the first eigenvector to construct the EDR wave [12, 31]. This is done because the relative position and amplitude of the peaks in the QRS complex is a direct consequence of respiration. This is because, as mentioned earlier, the signal read from the ECG contains an additive signal that reflects the shifted positions of the ECG leads due to the movement of the chest and is reflected in their amplitude. In addition, the position of these peaks iin relation to each other is a reflection of respiration, because respiration has been shown to directly affect the movements of the heart and thus change the temporal position of the peaks. All this information is processed by the PCA algorithm, which extracts the features

most relevant to the signal. Therefore, the first eigenvector containing the most important feature is selected to extract the respiration wave. The first eigenvector is found with the help of a singular value decomposition (SVD), where the first column of the U-matrix of the SVD corresponds to the column that contains the eigenvector with the highest eigenvalue and thus represents the first eigenvector. Since the PCA approach usually evaluates only the linear relationship between respiration and ECG, KPCA was developed to solve this problem and is therefore less suitable for short real-time data segments. Another disadvantage of PCA is that it performs poorly in the presence of noise and sudden changes in ECG data. [10, 37, 59, 73] are several research papers investigating this approach.

Although each of these methods takes a different approach to extracting the EDR waves, they have some steps in common, such as removing the DC frequency, filtering the very high and very low frequencies of the ECG signal, and in some cases applying a median and/or mean filter to remove unwanted signal components (e.g., Q and T spikes in the QRS complex). For better analysis, a cubic spline is often used to align signals with different frequencies, and detrend algorithms, applied on both the reference signal and the EDR, are also used to better visualize and filter the data. Although there is no universal method for preprocessing that should be performed for algorithms to improve performance, experiments show that some approaches, such as frequency-based, benefit from normalized signals, while others perform better with non-normalized signals (R-peaks).

It is also important to consider the various limitations of these approaches, such as the position of the electrodes [67, 73], age and gender [50], and the type of breathing, e.g., through the chest, that may affect the performance of the algorithms. Other aspects that may affect EDR extraction performance depend on the quality of the ECG [51]. However, it is almost universally accepted that noise and body motion negatively affect all methods and are difficult to eliminate completely in their entirety [57]. Therefore, other approaches are now being explored to replace or improve upon established algorithms, such as the use of neural networks, with some even using simpler networks that work alongside other existing methods [59].

2.3 A Review of Methods for EDR and Respiration Rate Extraction

In this section, we provide a more detailed analysis of the reviewed articles that serve as the basis for the methods implemented in this dissertation, which address both the extraction of respiratory waves from a respiratory signal and the extraction of EDR signals.

2.3.1 Determining the respiration rate

The state-of-the-art articles present in this subsection address the techniques used to determine respiration rate. Two main methodologies emerged: The first uses the frequency domain of the signal, the second the time domain. To conduct an investigation relevant to this dissertation, the methods examined focus on the use of either a IMU, a respiration sensor, or a combination of both.

Let us start with the study done in [42], in which the authors refer to a time-domain approach based on the detection of peaks and valleys in the respiratory wave. This detection of peaks is used to identify respiratory cycles, where a respiratory cycle is defined as two peaks in the data between valleys corresponding to two inhalations and one exhalation. To accurately distinguish these cycles, a threshold was empirically determined and implemented.

In order to test the adaptability and robustness of this method, a series of 4 controlled activities were performed in which subjects read aloud, smoked, and relaxed. The final results of this study showed an accuracy in estimating the correct respiratory rate between 85 and 99.6 percent compared to the manually determined respiratory rate. However, the fact that accuracy decreased when subjects did not relax suggests that body movement may be a source of error in correctly classifying respiratory rate. This and the lack of use of a commonly used database are the major weaknesses of this method. Nevertheless, this study proves that a time domain peak detection algorithm is very robust.

For an approach that now focuses on frequency domain analysis, the method [30] presented by authors P. Hung, S. Hood et al. serves as a good example. In this study, the authors perform a spectral analysis of the data collected by an accelerometer and a respiration band and extract the amplitude spectrum of the respiration waves. Using this spectrum, they were then able to determine the most important frequencies in the respiration wave and calculate the respiration rate. However, this method could only give a range for the respiration rate and not an exact value.

One method that uses both an inertial sensor and a time-domain peak detection approach is the study by M. Rahman and B. I. Morshed in [53]. In this study, the authors used a commercially tested respiratorysensor placed on the abdomen and a IMU device placed in the thorax. This allowed them to collect relevant information about a patient's breathing movements, regardless of whether the patient was breathing from the chest or abdomen. Once this data was collected, the readings were normalized in a vetorial configuration.

This representation allowed for more accurate detection of the peaks that make up the respiratory cycle. This proved to be effective, as the results showed a difference between the two detected respiratory rates of less than 2 bpm and 0 in most cases. However, this

study suffers from the fact that a protocol with fixed respiratory rates was implemented, which is not representative of a patient's normal breathing pattern, and from the lack of use of a common database for direct comparison. Nonetheless, the implemented algorithm has been shown to be robust when tested with real hardware, similar to that available for this dissertation.

Finally, concerning the computation of the respiratory rate, a conclusion in [5] is worth mentioning. This relates to the fact that noise and motion are still a major problem in monitoring respiration in studies with wearable sensors, as shown by the results of S. Beck et al. In their study, they implemented what is, as far as the author knows, a very rare approach in which the respiratory rate was determined based on the angular changes of two IMUs. This was possible because these angular changes are a direct result of respiratory motion. However, to accurately register these changes, a IMU device had to be placed on the patient's back to serve as a reference. This is not ideal because the sensor is in a very uncomfortable location for the patient. However, the results show that this configuration is a very stable method of correctly classifying respiratory rate. With the main drawback of this study being that only 5 data sets from no common database were used.

2.3.2 EDR extraction: Frequency based methods

Regarding the analyzed methods for direct extraction of an EDR wave, two articles are worth mentioning. While these articles are not specifically designed to present or compare a particular EDR extraction method, they do provide an overview of one or more EDR extraction methods and explain them in detail. Starting with [12], in which the authors focus on a detailed, summary, and consistent review of the most relevant studies available up to their publication in 2017. It explains how it is possible to extract a respiratory wave from an ECG signal (EDR) and explains the mechanisms of the most studied methods. This is a wonderful article for anyone interested in EDR, as it not only provides detailed explanations of the various methods, but also includes a number of other interesting articles.

Another article worth mentioning is [10], which is less general than [12] but is a very informative article in which the authors explain in detail in which areas of the ECG signal PCA can be applied. They explain that PCA is typically used to analyze the differences in amplitude and spacing between the peaks of the QRS complex, as these are a direct reflection of respiration. Also, other applications of PCA to the ECG are be presented in addition to EDR extraction, such as noise reduction techniques.

Thus, the remaining articles discussed in this section tend to focus on the correct extraction of an EDR wave, either as a final result or as an intermediate step.

Beginning with the article [31], in which the authors discuss the application of a Gaussian

filter to the ECG signal to filter out the respiratory wave contained therein. This article begins by defining a Gaussian process as a supervised learning method for solving regression and probabilistic classification problems that fits covariance functions to different ECG components. Therefore, the implemented algorithm focuses on estimating the hyperparameters of the GPs covariance function to extract the EDR signal using the GP specific transform and achieve proper separation between the EDR and the original ECG wave.

They test this approach with other state-of-the-art methods using a cross-correlation criterion. The result showed a cross-correlation of 70 to 72 percent in direct comparison with other methods, which ranged from 55 to 77 percent, with their bolk ranging from 60 to 77 percent. The authors therefore concluded that their method was on par with the rest of the state of the art. However, the complexity of the algorithm was not justified compared to the other methods, which did not perform significantly worse. Therefore, although this approach was used for comparison, it was not pursued further.

To investigate other filtering methods as well as other very well-studied EDR extraction methods, the article by J. Boyle et al. [7] was of interest. In this article, a combination of algorithms of bandpass filters, wavelets, and QRS are analyzed, giving a total of 6 methods. To test their performance, a metric was performed to evaluate the difference in the calculated respiration rate between the extracted EDR and the original respiration. The study concluded that the bandpass methods performed best, with the best results obtained with the bandpass filter between 0.2-0.8 Hz.

This proves that the frequency range of the analyzed frequency matters, as the other bandpass methods performed worse for other ranges. However, this does not mean that the other methods perform much worse. In fact, the DWT method outperforms the bandpass methods as the breathing frequency increases, while the QRS methods do not lag behind the others. This proves that the implementation of multiple EDR extraction algorithms might be necessary, as their performance can be comparable, with some methods adapting better to certain scenarios.

As for the other frequency-based methods presented in [7], the DWT can be further explored in [62]. In this study, the authors use the DWT property of applying successive low-pass and high-pass filters to decompose a signal into a series of coefficients representing the numerous signals contained in the ECG by their frequency. Then, by applying an inverse DWT to the coefficients containing the signals whose frequency matches that of respiration, an EDR is created. To test this implementation, the authors then apply a metric that evaluates the difference between the respiration rate of the EDR and the original respiration signal.

The results show that there is a small error between the respiration rate derived from the

EDR signal and the original respiration rate. Therefor indicating that the EDR wave must contain similar information as the original respiration wave. This confirms the assumption that the DWT method can be successfully used to extract an EDR signal. In addition, they use the widely available Fantasia database, which allows for a more direct and accurate comparison with other methods.

2.3.3 EDR extraction: QRS complex analysis methods

At this point in the review, however, it became clear that frequency-based methods are susceptible to various forms of error and are highly dependent on the frequency band in which they operate. Therefore, an investigation of the very common analysis of the QRS complex, see Fig. 2.2, was undertaken.

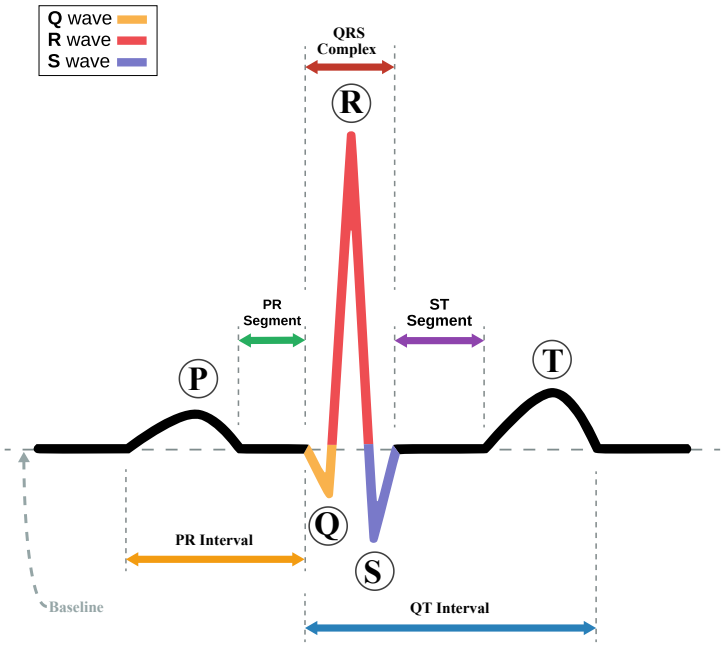

Figure 2.2: Standard QRS complex configuration [2].

Let us start with the multiple-method case study proposed by E. Helfenbein et al. in [29], which takes into account both respiration-related changes in the amplitude of the QRS peaks and heart rate, as well as an innovative method that uses the effects of muscle movements associated with respiration to obtain an EDR wave. The first two methods start with the detection of R peaks in each QRS complex and then focus on the changes in amplitude and temporal position of these peaks to extract EDR waves.

To this end, the authors use a cubic spline interpolation to generate the EDR signals, assuming that the amplitude changes and the interval between the peaks correlate with the respiratory waveform. However, the most innovative and interesting method was the EMG method, which is based on the fact that a very highly sampled ECG signal of at least 500 Hz contains information about muscle activity associated with respiration. However, since the sampling rate required for this method is much higher than that of the ECG available for this dissertation, it will not be discussed further.

With this in mind, the results of the two remaining algorithms that compared respiratory rate to each other and to the ground truth proved to be sufficiently free of error to warrant their pursuit.

Difference in amplitude and interval of the QRS complex peaks as a direct consequence of respiration

Therefore, to gain a better understanding of the possibilities and limitations of methods based on the study of the QRS complexes, a more in-depth analysis is needed. Therefore, the next articles will focus on the direct changes in the amplitude and interval of the R peaks as a direct consequence of respiration.

Using the study by J. Kim et al. compiled in [36] as a starting point. In this study we can see that the assumption that the temporal information of the ECG varies with respiration in terms of the placement of the peaks is reliable for the extraction of the EDR signal. Not only that, but that this can be done in a variety of ways. This was demonstrated by the authors, who implemented both the evaluation of the area under each R-peak, since this area directly reflects the inhalation or exhalation motion, and the difference in the interval between R-peaks. However, no information was presented on the performance of the algorithms, except that direct visual evaluation of the waves showed that the extracted waves were similar to the original respiratory waveform.

However, in [76] a concrete comparison is made between different state-of-the-art methods based on the cross-correlation metric. In this study by A. Zarei and B. M., the Ramp, RSamp, and QRS methods are compared with two new EMD methods proposed by the authors. Although the goal of this study is to automatically detect OSA, an in-depth comparison is also made in terms of extracting the EDR from the different methods. The results show that all algorithms have a mean cross-correlation of about 68 to 79%, with a slightly higher median value. In the tests performed, the Ramp algorithm is the better method in terms of score, proving the effectiveness of the algorithms based on the analysis of the QRS peaks compared to the state-of-the-art methods. It was also shown that the EMD methods can produce EDR waves similar to the original respiratory waves. However, the EMD methods

presented required a high computational cost that could not compensate for their more robust performance compared to the other methods, with the authors even acknowledging that their algorithms are not applicable in a real-time scenario.

Extraction of the spacial features or respiration in the QRS complex that reflect the respiration with the use of PCA

It has been shown above that analysis of the QRS complex is not only viable, but can outperform other modern methods depending on the scenario. However, there are other ways to analyze the respiratory information contained in the QRS complex. To this end, PCA algorithms are used to extract key features in the QRS complex that are related to respiratory motion.

A practical application of PCA to the QRS complex is the method developed by P. Langley et.al. [37], which achieves high values in cross-correlation even compared to other state-of-the-art algorithms tested. This was demonstrated in this study, in which 14 methods were tested, including the Ramp method and the R-Interval method. The results of the cross-correlation metric showed that the results of the PCA algorithms were more stable and less error-prone than those of the reference methods. In addition, they were able to achieve a mean correlation value of 73 to 80 percent, depending on which PC was extracted and for which input. However, the use of a protocol with fixed breathing patterns does not represent the condition of a patient on a normal day. This and the fact that no commonly available database was used proved to be the major weakness of this study.

Another interesting paper on the use of PCA is described in [73]. where the authors investigate the use of a kernel function before applying the PCA algorithm. This method, known as Kernel PCA (KPCA) can be considered a general extension of the PCA algorithm, where non-liniarities in the data are taken into account. This is achieved by using a kernel function that maps the raw input data to a higher dimensional level, as there are sometimes features that can only be seen in this type of representation, to which PCA is then applied.

The authors tested the KPCA algorithm with different hyperparameters and compared their results with the Ramp method using the cross-correlation metric. The results show that the tested algorithms have an average cross correlation of about 70-76%. It was also found that the method with the lowest result was the Ramp method, whose average cross-correlation value was in the range of 50%, proving that the performance of this method can vary greatly depending on the scenario. However, the better performance of the KPCA algorithms was associated with high compatibility costs. Therefore, this method is not investigated further since other methods implemented in the Fantasia database, including normal PCA, provide performance in the same range as KPCA.

2.3.4 EDR extraction: Empirical Mode Decomposition analyses

In this last phase of the review, the EMD methods are analyzed. This is done because this method has been shown to achive high performance when applied to the cross-correlation metric in [76] and is also a widely studied method. Stariting on the work of K. V. Madhav et al. [45], which serves as a good introduction to the structure of EMD algorithms and shows how they can be used for EDR extraction. A visual example of how the EMD algorithm extracts the individual IMFs that comprise an signal can be seen in Fig. 2.3.

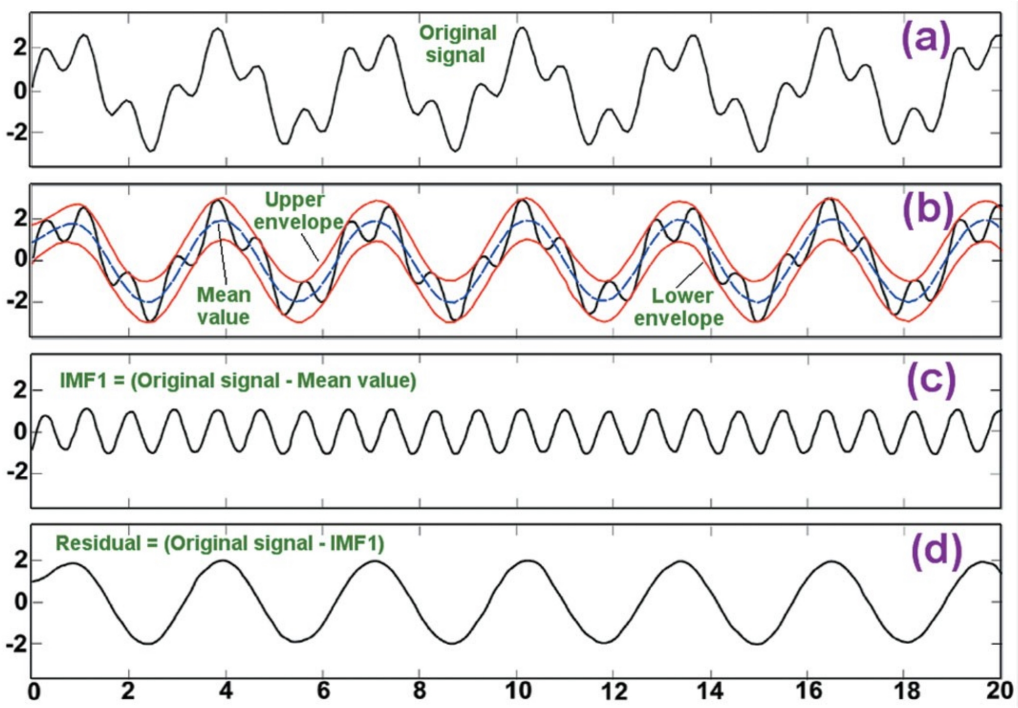

Figure 2.3: Standard example of how an EMD algorithm extracts the IMFs of a signal [58]. In section a) you see the original signal. An upper and a lower envelope are then fitted to this signal, from which the average of both envelopes is calculated, as seen in section b). This average contains information about the signal with the highest frequency present in the original signal. Therefore, it is possible to extract this high frequency signal by subtracting the calculated average (see c) from the signal in a). This residual, present in d) is then subjected to a series of criteria to determine if it corresponds to an IMF. If it is not, the procedure is repeated until it is. After the IMF is correctly found, it is removed from the original signal. The resulting signal is then used to extract the second IMF by performing the same procedure until all IMFs have been successfully extracted.

In this study, the authors provide a pseudo-algorithm as a "template" for the general structure of the EMD and show how they extract the IMFs. After a detailed explanation of how the model used works, both cross-correlation and respiratory rate error metrics were applied to test its performance. The results for the EMD algorithm in the cross correlation

metric showed an amazing mean cross correlation of over 90%. This not only makes this EMD algorithm the highest scoring method in the cross correlation reviewed, but also supports the idea that EMD methods are capable of extracting EDR waves that are very similar to the original repsiratory waves. However, it is worth noting that the algorithm tested in this study did not use the full extent of the Physiobank database MIMIC and was tested on only a few subjects, which may have affected the results.

Another approach to using the EMD method that has attracted interest and has been referenced in numerous other studies is the EEMD algorithms. These algorithms use the ML technique of ensembles and its premise of "more minds think better than one" to achieve better performance. These methods achieve this by using a subset of the data to train an ensemble of EMDs and adjust the EMD hyperparameters. Thanks to this approach, the EEMDs are then able to obtain the best output for their EMD configuration. The result is a method that is both capable of extracting the EDR wave that is most similar to the original respiratory wave and is a method with high performance and robustness.

However, this comes at a cost, as not only is a training procedure required, but also the fact that the EEMD is inherently ensemble. This is illustrated by the study of K. T. Sweeney et al. in [69], in which an additional white noise step was performed in each independent EMD algorithm. The results show both the advantages and disadvantages of the EEMD architecture, as a very efficient, robust, and noise-resistant method was created (thanks in part to the additional white noise), but at the cost of very high computational power.

Therefore, it was concluded not to use the EEMD approach, since the performance was not significantly better than that of the regular EMD algorithms and this increase did not justify the very large increase in computational power, which is a major drawback for use in a real-time system.

2.4 Literature Gaps and Statement of Contributions

In this section, we attempt to identify some of the key gaps found in our review of the current state of the art, as well as highlight the contributions of this dissertation.

One of the major gaps in the current state of the art regarding the use of multiple sensors for health issues is that the systems studied are usually used for very specific circumstances. That is, and as far as the author is aware, most techniques have been used for very targeted applications and have not taken full advantage of multi-sensor fusion. Another drawback of current approaches is the use of multiple sensor types that focus on only one aspect, such as using different sensors to classify posture without considering a broader range of features. This could be addressed in a number of ways, such as using the information collected and

processed by the different sensor modules and merging their data at a higher level to gain a deeper understanding of how the systems they are used in work, or simply using the same sensor to draw different conclusions. In this way, it may be possible to improve the accuracy and robustness of measurements while minimizing the use of sensors for the same set of signals.

Other limitations of the current state of the art include the fact that many broad studies on this topic rely on databases that are not always widely and freely available. Alternatively, their approaches focus on a particular group or set of conditions, making the results obtained in these studies less representative, leading to more targeted approaches whose performance may vary widely in an unknown scenario. This leads to uncertainty about which algorithm performs best in a given case, with some performing differently even based on the given data. This makes it unclear which algorithm is the most robust overall [12]. Another major problem is that the results presented are only the best possible results and in some cases omit data that would affect performance [37, 50]. Another major drawback of some studies is that they only tested their methods with simulated data, which makes it difficult to evaluate the performance of the algorithms in real-world scenarios [62].

Our contribution, therefore, is to develop a consistent and robust continuous monitoring system for patients that will improve their overall satisfaction and increase their freedom and physical comfort when continuous monitoring of their vital signs is required. To this end, this dissertation focuses on the use of real data obtained from regularly available and intensively studied databases, as well as data collected by a belt developed within WoW, which encompasses several different sensors, including the dedicated respiratory sensor and ECG to monitor the patient's respiratory data. Therefore, this dissertation investigates a respiratory rate algorithm in combination with different EDR extraction methods. This makes it possible to apply the respiratory rate algorithm not only to the data collected by the dedicated respiratory sensor, but also to the EDR waves extracted from the ECG. Both sensors can be used to increase the accuracy and robustness of the respiration rate, while continuously monitoring a patient's breathing even if one of the sensors fails.

3 Methodology and Implementation

In this chapter, the algorithms implemented in this dissertation to calculate the respiration rate and the different EDR extraction techniques are explained.

3.1 Extraction of respiration rate with a peak detection approach

Let us start with the method of classifying a patient's respiratory rate, which ranges from 12 to 18 breaths per minute in adults [63]. This method is based on the assumption that a complete respiratory cycle (inspiration and expiration) results in two maxima and one minimum in the data of a respiratory wave. This is done to count the number of complete respiratory cycles in the analyzed data window, since it is possible to truncate a respiratory cycle when a number of x seconds of respiratory data is selected, so that only the complete sets are considered. In the case of this dissertation, this is possible due to the elasticity of the respiratory sensor, which changes its internal electrical resistance as it is stretched and contracted. This produces an electrical signal that resembles a waveform very similar to thoracic displacement. In this way, a graphical representation of a person's inhalation and exhalation is created, as shown in Fig. 3.1.

However, the sensor used is very sensitive and therefore detects a large amount of noise, such as the movement of the body when walking/running or changing posture, as well as other, more subtle signals. These more subtle signals result from normal body movements, such as the heartbeat, which causes noise when the patient is breathing at a very low frequency. However, the source of the noise can also be caused by the belt itself, such as when the battery of the belt vibrates in thinner people or asthmatics because it does not rest firmly on the chest, creating an artificial vibration. This would not be a major problem if the patient simply breathed in a stable position with a normal breathing rhythm, as in Fig. 3.2, where almost all peaks correspond to a true inspiratory movement. However, this is not possible because high-frequency signals must be considered during a faster breathing cycle or during speech, even when the position is stable, as in Fig. 3.3 . In this figure most of

the small peaks correspond to real inhalation and exhalation movements that at first glance would be considered noise, making the elimination of noise in the data very difficult.

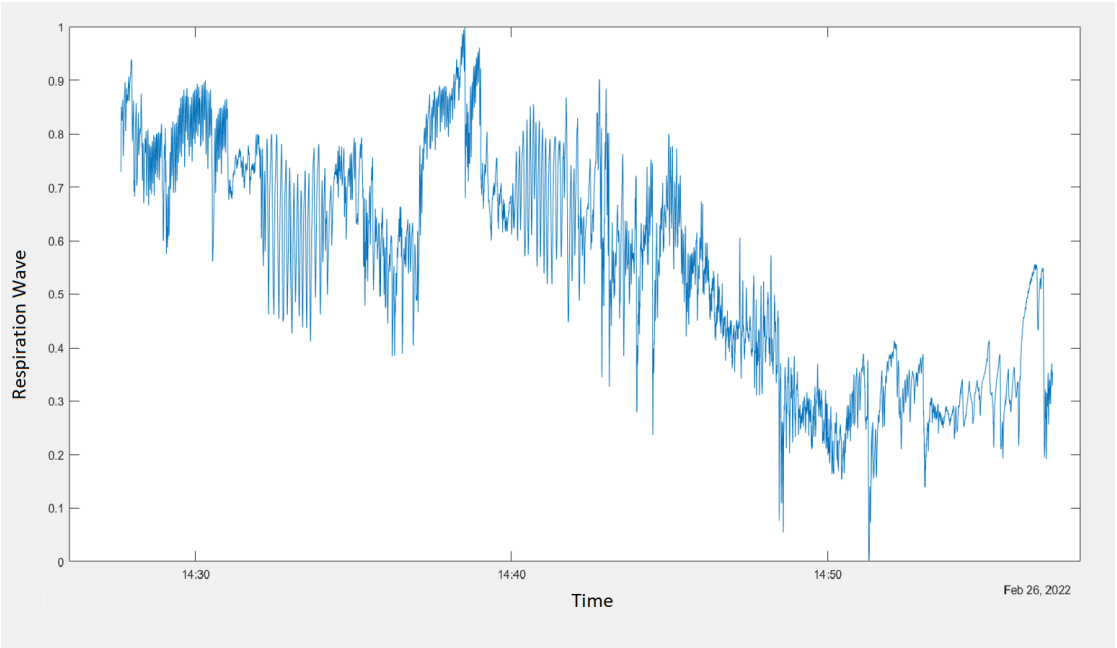

Figure 3.1: Normalized data for a scale between 0 and 1 recorded by the respiratory sensor in a variety of positions and respiratory rates. The X axis corresponds to the time in hours at which the data was recorded, and the Y axis is the amplitude of the electrical signal obtained from the bed.

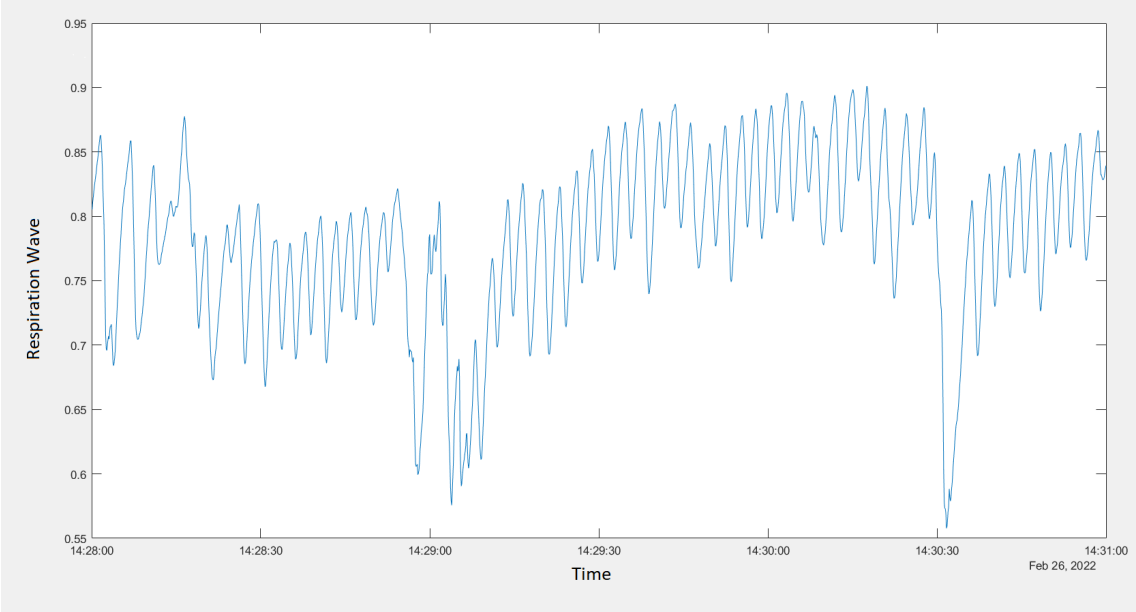

Figure 3.2: Normalized raw data,for a scale of between 0 and 1, collected from the respiration sensor in a sitting position with normal respiration rate.The X axis corresponds to the time in hours at which the data was recorded, and the Y axis is the amplitude of the filtered signal.

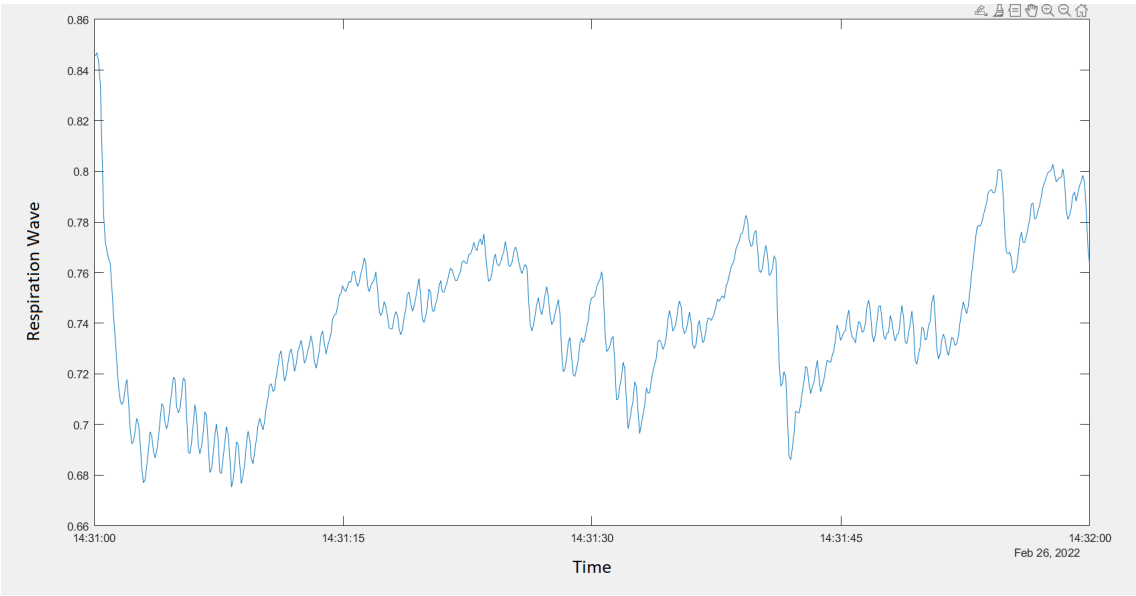

Figure 3.3: Normalized raw data collected, for a scale between 0 and 1, from the respiration sensor in a sitting position with fast respiration rate. The X axis corresponds to the time in hours at which the data was recorded, and the Y axis is the amplitude of the filtered signal.

7

However, some of the small peaks correspond to noise. Therefore, a low-pass filter of 2.5 Hz was used to ensure that most of the recorded data matched the actual respiratory motion. This frequency was chosen because it gave the best result of all the frequencies

tested. However, this low-pass filter was not sufficient to produce a sufficiently clean signal. Therefore, to improve the signal while accounting for the higher frequencies of respiration, a Savitzky-Golay filter is used. The Savitzky-Golay filter is often used to smooth digital data because it monitors the signal without much delay and preserves the high-frequency components by polynomially estimating a wave that retains most of the signal's original information. This is extremely useful for calculating a higher-frequency respiration rate because noise generated by motion can be removed while preserving the overall structure of the wave. Thus, after a series of systematic tests on the data, it was concluded that a Savitzky-Golay filter with a window of 29 data points (about 30s) with an approximation function of order 12 gave the best results and was therefore selected. These filters are then applied to a buffer containing information about the last 30 seconds of data. The result is a buffer of filtered data to which three fixed-size windows of 5, 8, and 15 seconds are then applied. In this way, a more accurate respiration rate is calculated that quickly adjusts to the respiration rate.

The reason for choosing this 3-window approach is that each respiratory rate tested has a different number and shape of respiratory cycles, with these cycles corresponding to 2 maxima and 1 minimum (max-min-max). For example, at a faster respiratory rate, the respiratory cycles would be smaller in amplitude and closer together. To account for these differences, 3 different sized windows are implemented for a given respiratory rate, i.e., slow, normal, or fast, each of which calculates a respiratory rate value that is selected based on a set of rules to determine the most accurate respiratory rate in a given scenario. Therefore, the respiratory rate is calculated in breaths per minute according to the following formula:

$$respiration\_rate = 60 * (number\_of\_respiration\_cycles)/(second\_of\_window) \quad (3.1)$$

Regarding which breathing rate is considered the most accurate in this 3-window approach, the following rules are applied: First, the 5-second window is applied, and if the respiratory rate is greater than 25 bpm, it is selected as the most likely respiratory rate because the peak values of the faster respiratory rates are close to each other. This is an advantage for faster respiration rates that the 8-second window does not have, as it would consider a larger portion of the data, resulting in a respiration rate that is not indicative of the actual respiration rate. Therefore, after checking the values of the 5-second window and if the respiration rate selection criterion is not met, the algorithm calculates the respiration rate of the 8-second window. If the respiration rate of the 8-second window is higher than 10 bpm, the respiration is considered normal and this respiration rate is selected as the final respiration rate of the system. However, if the respiration rate calculated for the 8-second

window is less than 10 bpm, it means that the respiration is slower and the peaks are far apart. Therefore, the 15-second window is used because the 8-second window is not able to calculate this respiration rate correctly because most of the information is out of its range. The entire procedure for calculating the respiration rate can be seen in the pseudocode in Algorithm 1 and a visual representation of this algorithm can be found in Fig 3.4 .

It was visually confirmed on a graphical interface presenting the data received by the sensors of the belt, that this approach is able to accurately switch to the smallest window when the respiration rate is increased. This updates the respiration rate in a useful amount of time and provides a more accurate respiration rate for higher frequencies. This is also true for the larger 15-second window, as it can correctly calculate the lower respiration rate with the largest amount of data than the 8-second window, as it would take incorrect values.

However, this approach is mostly limited to stable positions and pure breathing, because when the patient is in motion, it becomes more difficult to eliminate the false peaks. To combat these issues, methods capable of extracting a respiratory signal from the ECG to provide a secondary data source are also being used.

Algorithm 1 Respiration rate calculation algorithm

loop
- Get **new** data form sensors
- **Update** buffer
- Apply **2.5 Hz** low-pass filter
- Apply **Savitzky-Golay** filter
- Run **5, 8 and 15** second windows on the filtered buffer
- bpm_5s is the respiration rate in the 5-second window calculated in bpm
- bpm_8s is the respiration rate in the 8-second window calculated in bpm
- bpm_15s is the respiration rate in the 15-second window calculated in bpm
- F_bpm is the chosen respiration rate
- **if** $bpm\_5s > 25$ bpm **then**
  - $F\_bpm \leftarrow bpm\_5s$
- **else if** $bpm\_8s < 10$ bpm **then**
  - $F\_bpm \leftarrow bpm\_15s$
- **else**
  - $F\_bpm \leftarrow bpm\_8s$
- **end if**
- **Update the current** respiration rate as F_bpm

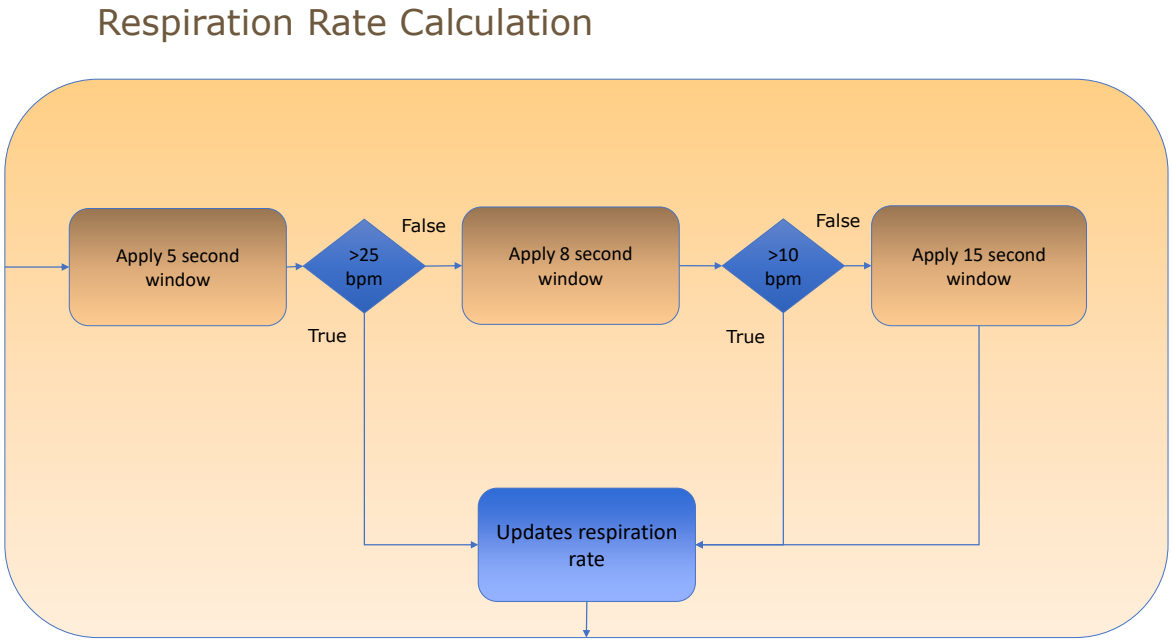

Figure 3.4: Visual representation of the respiration rate algorithm using a 3 window strategy.

3.2 Extracting EDR signals from an ECG

In this study, eigth techniques were implemented that correspond to the most common and studied EDR techniques. They were also chosen because they best fit the project in which this dissertation is embedded. In the remaining of this section we provide an explanation as to which methods were implemented and how.

Fast Fourier Transform (FFT). The purpose of this method is to remove from the signal all frequencies outside of the respiratory frequency, which in this study was between 0.05 Hz and 0.66 Hz. This range was chosen to account for a wider range of possible respiratory frequencies. While it was found experimentally that narrowing this frequency band to a frequency closer to the actual respiratory frequency of the signals improved performance. This was not done because it limited the range of the algorithm and required prior knowledge of the breathing frequency, which defeated the purpose of EDR extraction. However, the results obtained with this method were always above the 80% correlation threshold, so this was not considered detrimental for practical applications. Where for the transformation of the ECG data to the frequency domain the **numpy.fft()** function was used.

Discrete Wavelet Transform (DWT). In this method, the Python function ***pywt.dwt()*** from [40] was used to calculate the decomposition coefficients of the input signal after a user-defined function determined the number of decomposition stages. This was done due to the

fact that the required decomposition levels change depending on the ECG sampling rate. After selecting the correct decomposition coefficients that fall within the frequency range of respiration, the inverse DWT was applied to them to generate the EDR signal. The wavelet *db2* was selected because it had the highest correlation values among the tested wavelets, as it best matched a normal respiratory wave.

State-of-the-art NeuroKit2. This EDR extraction method is one of the methods included in the Python package NeuroKit2 [46], which was used in this dissertation as a means to compare the other methods with a tested EDR extraction method. This particular library was chosen because it is capable of automatically extracting an EDR signal from an ECG input signal and sampling frequency without requiring any knowledge of EDR extraction. Another factor that led to the use of this particular Python package is that it also has a built-in R-peak detection function that can be used individually and independently in the code. This has proven useful as this R-peak detection function is a fast and accurate R-peak detection algorithm, especially when compared to other tested R-peak detection algorithms that have similar peak detection performance, but in most cases at the expense of computation time. The specific soni2019 EDR extraction method included in the Neurokit2 library was selected because it performed best on the data tested. This method is based on an algorithm capable of finding the frequency peaks of an input signal and after selecting the frequency peaks that fall within the range of the breathing frequency, a bandpass filter is applied with a cutoff frequency based on these peaks. Therefore, for the purposes of this dissertation, this method will be referred to as NK2S19, as an abbreviation for NeuroKit2 soni2019 method.

Empirical Mode Decomposition (EMD). The extraction of an EDR signal using an EMD method was performed using the Python EMD toolbox [52]. This toolbox is able to extract the IMFs present in an input signal, in this case the filtered ECG, and returns them in an array, where the first element corresponds to the IMF with the highest frequency. After the IMFs were extracted, a Hilbert-Huang transform was used to determine their individual frequency. After the frequency of the IMFs was correctly determined, the IMFs whose frequency was within the breathing range (0.05 Hz and 0.66 Hz in this study) were combined to obtain the extracted EDR wave.

QRS peaks amplitude based methods. As for the study of changes in the peaks of the QRS complex derived by the respiration, the methods used in this dissertation are based on changes in the amplitude of the R peaks due to lung movements. These methods were chosen because they provide more robust and accurate results in experimental comparison

with the interval-based methods. Therefore, two approaches to this method are implemented, differing in that the Ramp method calculates the amplitudes of the peaks with respect to a baseline of the signal, while the RSamp method calculates the amplitudes between the R peak and the S peak, where the S peak is the minimum point immediately after the R peak.

PCA. The PCA algorithm used in this dissertation is based on the BioSigKit toolbox [64], originally developed in Matlab and intended for biosignal analysis. In this toolbox, the EDR is extracted by applying PCA to the data centered around the R peaks and using the first eigenvector to construct the EDR wave. To use this method in Python, an adaptation of the original PCA algorithm was made. In this method, multiple windows of data centered around the detected R peaks in the input ECG are extracted and fed to the adapted PCA algorithm, from which the first eigenvector is extracted using SVD and interpolated to generate the EDR signal. However, it is worth noting that the PCA algorithm cannot be used properly if there are less than 2 R peaks in a given ECG input signal, so the EDR signal is returned as a flat line. For this method, 2 approaches have been implemented. In the first approach, the raw ECG data are used to detect the R peaks and used as input to the PCA algorithm. This approach is referred to as Adpated PCA or APCA for short. In the other approach, a 200ms and 600ms median filter is applied to the ECG signal before the R-peaks are extracted, and the filtered ECG is used as input to the PCA algorithm, which is why this approach is also referred to as Adapted PCA filtered method or APCAF for short.

To test the EDR extraction methods, they are applied to a set of individuals from two databases: the Fantasia database of Physionet [24], which contained both ECG and respiratory signals, using the latter as ground truth. Data from this database were sampled at a frequency of 250 Hz. The subject population was well represented in both younger and older subjects and was evenly distributed with respect to sex. The other database used was the Medical radar database [13], which also contains ECG and respiratory signals but at a sampling rate of 1000 Hz. Its subject population focuses on younger adults aged 24-25 $\pm$5 years (5 men and 4 women). This database was also chosen because it could be used to create variation in the datasets tested and to determine if very high sampling rates would affect performance, since the ECG is normally sampled at 200-250 Hz. The lower sampling rate was investigated in the validation data from the WoW project belt. Another advantage in selecting these databases was that they have both been used in articles on EDR extraction, such as [13, 31, 73, 76], with the Fantasia database being used widely in the literature.

To simulate real-time behavior, a sliding window of 30 seconds was applied over the entire length of the signals, and the eigth EDR extraction algorithms were applied to the

window every 2 seconds. This resembled a real-time system in which EDR wave extraction is performed at a regular, fixed interval to reduce computational overhead. In each 30-second window, both the respiratory signal and the corresponding ECG signal were filtered. In the case of the respiratory signal, the DC component was removed by removing the average of the original signal and normalizing it. This was followed by a 0.7 Hz low-pass filter and a Savgol filter of order 6 and a sampling window of 19 data points. These values were chosen because they provided the best results for the range of values reported in the literature that were experimentally tested in this dissertation. Finally, a detrend function was applied to facilitate comparison of the results.

The treatment of ECG signal data depended on whether or not the method used was based on analysis of the QRS complex peaks of the ECG wave. This was because it was empirically found that the QRS methods used performed better without most of the preprocessing. Thus, for the QRS based methods, a 200ms and 600ms median filter was applied to the signal to remove the P and T waves, respectively [73]. For all other methods, a notch filter was applied to the 50 and 60 Hz frequencies to remove network noise and baseline wander [51]. Then the DC component was removed by subtracting the mean of the signal, followed by a median filter, detrend function, and normalization. For a diagram showing the experiments performed in this dissertation, see Fig. 3.5.

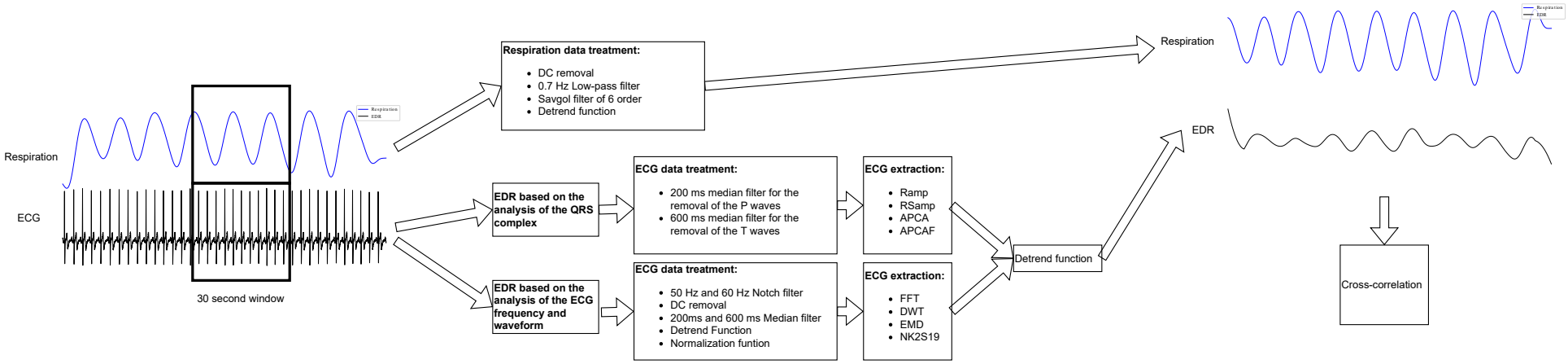

Figure 3.5: Diagram of the EDR extraction process, with a sliding window running through the data. Every 2 seconds, the data within the window is filtered and used to extract an EDR wave using the method described in the figure.

4 Experimental Validation

4.1 Peak detection algorithm with data treatment

To test this algorithm on the belt of the WoW project, a relevant dataset was collected from it, in the configuration present in Fig. 4.1 where both used respiratory and ECG sensors and their positions are labeled. For this dataset the subject wore the belt and breathed and spoke in four different postures - sitting, standing, walking, and laying- with three different breathing rates (normal, fast, slow) recorded in Table 4.1. This was done to ensure that a wide range of meaningful data was collected so that the algorithm could be tested more extensively under different circumstances and its response to each circumstance could be analyzed more thoroughly.

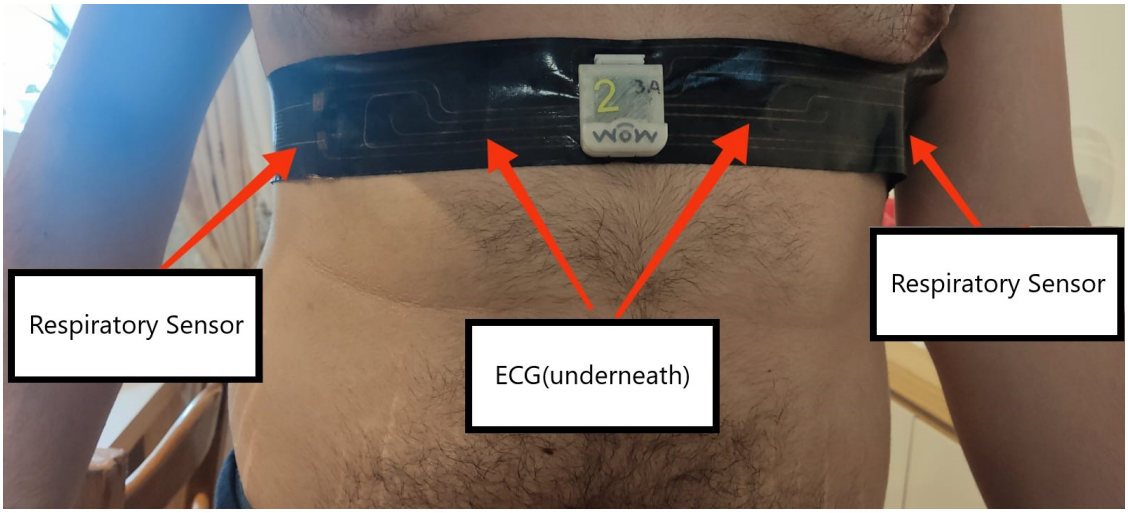

Figure 4.1: WoW project belt for monitoring respiration. In the figure, the sensors relevant to this dissertation are marked and labeled. Namely the respiratory and ECG sensors.

The results of implementing the respiratory rate classification algorithm described in 3.1 show that the calculates values match with the counted respiratory rate for each sector. This is especially true for the more stable positions such as sitting and standing, except during a

Position	Breathing Method	Start Time	End time
Sitting	Normal	14:28	14:31
Sitting	Fast	14:31	14:32
Sitting	Slow	14:32	14:34
Sitting	Talking	14:34	14:37
Standing	Normal	14:37	14:39
Standing	Fast	14:39	14:40
Standing	Slow	14:40	14:42
Standing	Talking	14:42	14:44
Walking	Normal	14:44	14:46
Walking	Fast	14:46	14:47
Walking	Slow	14:47	14:49
Walking	Talking	14:49	14:51
Laying Down	Normal	14:51	14:53
Laying Down	Fast	14:53	14:54
Laying Down	Slow	14:54	14:56
Laying Down	Talking	14:56	14:57

Table 4.1: Breathing position and rates as measured by the belt, along with their respective times.

conversation, as shown in Fig. 4.2. In these figures, it is easy to find the zones of fast and low breathing rate in the data set corresponding to the same periods recorded in 4.1.

However, it should also be noted that it is very difficult to distinguish between the different breathing rates between the times 14:44 and 14:51 corresponding to the walking segment of the data. Here, although there is a relative difference between the normal fast and slow breathing rates, it is not clear whether the higher values are a direct result of the faster breathing caused by the increasing activity or whether they are the result of the noise caused by walking. As in fig. 4.3, it is very difficult to distinguish between true peaks corresponding to respiration and those generated by noise. In fact, most peaks that at first glance one would think are noise correspond to true peaks.

This is problematic because the respiratory sensor can detect more subtle movements caused by normal body movements, such as heartbeat, resulting in noise, especially at lower respiration rates. However, some of the noise is also caused by the belt itself, for example when the belt's battery vibrates in thinner or asthmatic people because it does not rest firmly on the chest, creating an artificial vibrating motion.

As for the shape of the filtered respiration waveform itself, one can see in Fig. 4.4 that some of the noise and false peaks have been corrected compared to the low-pass filtered data in Figure 4.3. This not only attenuated some of the noise, but also removed some of the false peaks that can occur when a patient inhales twice.

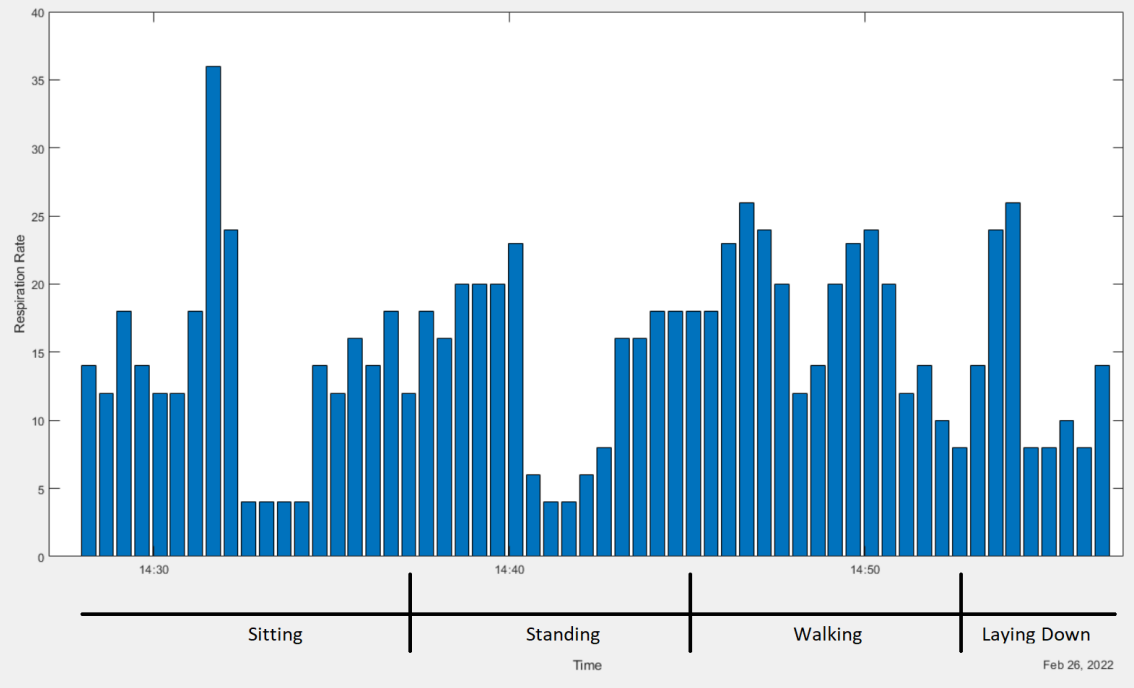

Figure 4.2: Calculated respiration rate every 30 seconds using the peak detection method. The X-axis corresponds to the time in hours interval of the data and the Y-axis represent the computed respiration rate.

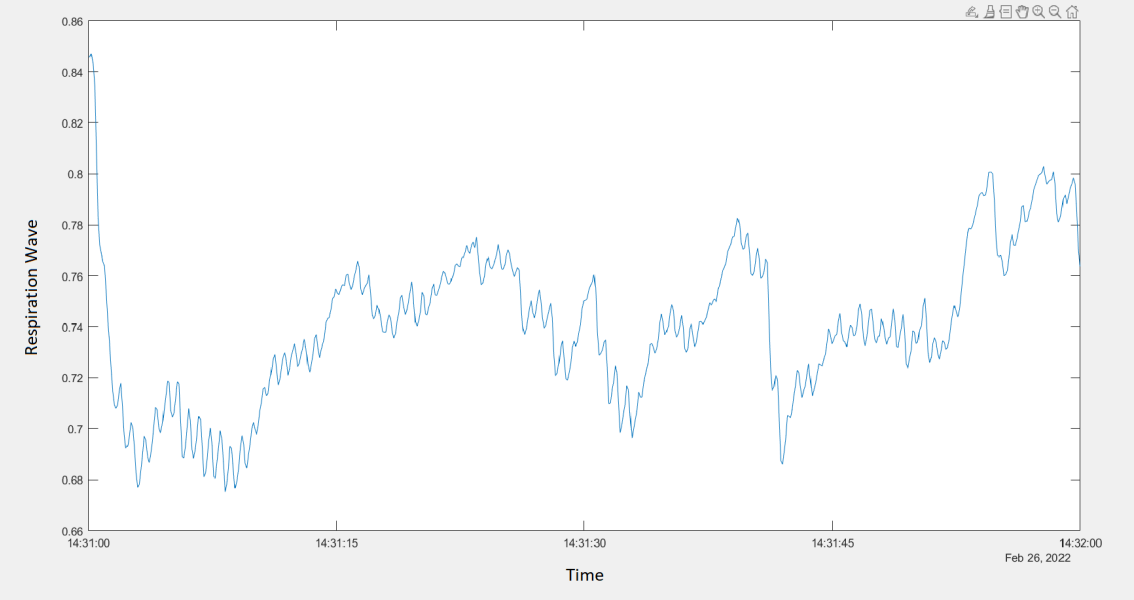

Figure 4.3: Filtered data with a low pass filter of 2.5 Hz of the sitting position whit fast breathing.The X-axis corresponds to the time in hours interval of the data and the Y-axis represent the filtered signal.

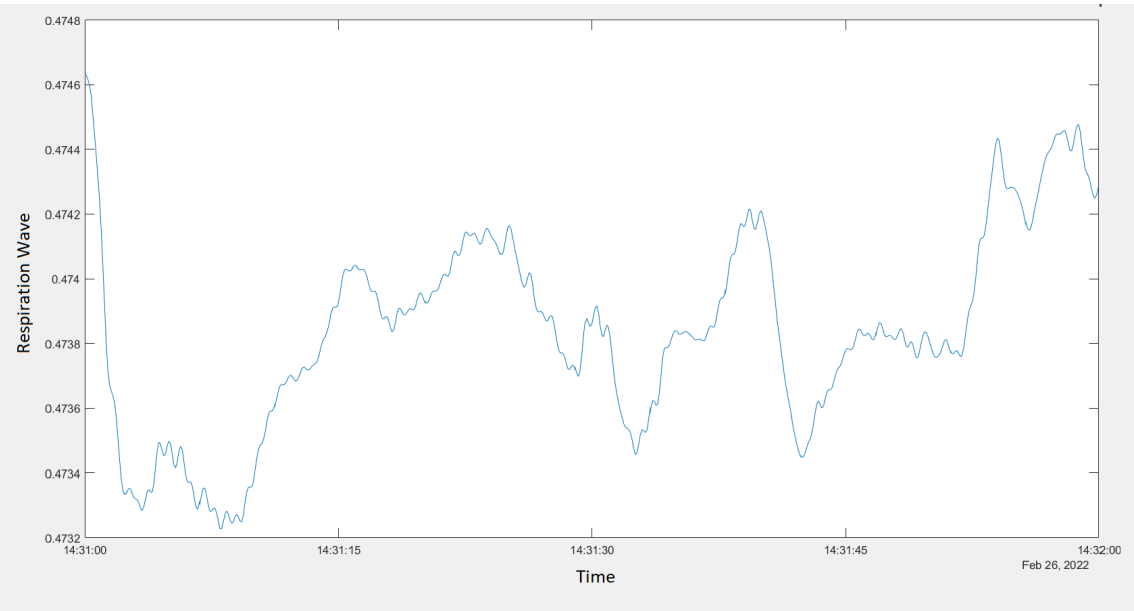

Figure 4.4: Filtered data with the Savitzky–Golay filter of the sitting position for fast breathing. The X-axis corresponds to the time in hours interval of the data and the Y-axis represent the computed respiration rate.

This algorithm was also tested in real-time where it has been visually confirmed that the 3-Window approach is able to accurately switch to the smallest window when the respiration rate is increased. This updates the respiration rate in a useful amount of time and provides a more accurate respiration rate for higher frequencies. This is also true for the larger 15 second window, as it can correctly calculate the lower respiration rate with the largest amount of data than the 8 second window, as it would assume incorrect values.

4.2 EDR extraction from ECG signals

To evaluate the performance of the implemented EDR extraction algorithms, two evaluation criteria were implemented. This was done on a dedicated computer that applied the methods explained in the previous section to the integrity of the databases. The first evaluation criterion implemented was the **cross-correlation** function between the respiratory signal, which serves as ground truth, and the extracted EDR signals. This was done because the cross-correlation function, when normalized, indicates the similarity between two signals even if there is a temporal shift. For this purpose, we use a cross-correlation function based on the following formula:

$$\widehat{R}_{xy,coeff}(m) = \frac{\widehat{R}_{xy}(m)}{\sqrt{\widehat{R}_{xx}(0)\widehat{R}_{yy}(0)}} \tag{4.1}$$

Where R_{xy} corresponds to the values of the cross-correlation between the extracted EDR

and the original respiratory signal, $R_{xx}(0)$ is the maximum value of the autocorrelation function of the respiratory signal, and $R_{yy}(0)$ is the maximum value of the autocorrelation function of the EDR signal. This particular function was selected as the first evaluation criterion based on two points. First, this function is able to return the cross-correlation in normalized and non-normalized form. The reason for this is that this function is often used to detect signals that are sent over long distances and may have amplitude and phase shifts. In this type of application, it is sufficient to find the timestamp in the received signal that has a higher value of autocorrelation to detect the original signal.

However, there are cases, such as the one in this dissertation, where it is not enough to assess the temporal difference, but it is also important to determine how well they match. To this end, the chosen function can adjust its formula to match the formula shown in 4.1 by specifying it with the flag *'normalized'*. This function then returns a percentage in the interval between 0 and 1, indicating the extent to which our extracted EDR signals resemble the original respiratory wave.

Another aspect that has contributed to the use of the cross-correlation function is its ability to accurately compare two signals even if they have a phase shift. This is important because some methods can easily shift the waveform during the extraction of the EDR signals, such as the FFT method. For this purpose, we compute the value of the cross-correlation between the ground truth and the time-shifted EDR signal for all possible positions and returns a vector with the cross-correlation values for all these positions. Finding the highest value in this vector determines the true value of the cross-correlation.

The second implemented evaluation metric refers to the **computation time** of the methods measured in seconds. This information is crucial as it can show us whether a method is suitable for use in real-time applications or not, given the fact that in this sorts of applications, where multiple algorithms are executed in parallel, the computation time has a major impact on the performance of the system.. To this end, two time evaluations were performed when applying the EDR algorithms to the databases. The first refers to the time it took the computer to filter and extract an EDR wave from a 30-second window, as this would reflect the performance of the algorithm in a real-time system. To this end, a timer was set to the moment the algorithm extracted the ECG signal and stopped only when the EDR wave was fully extracted. The second time reference examined refers to the time it took each method to fully analyze a subject's data. To this end, a timer was set when the data was loaded from the subject and stopped only when the program ended. For this purpose, all algorithms were tested on a computer whose hardwere specifications are: Asus PRIME Z590-P motherboard with an Intel i9 11900KF 3.5Ghz 8-core, 64GB RAM (DDR4) and Nvidia RTX 3080 Ti.

For a more detailed discussion of the EDR extraction algorithm results for each evaluation

criterion, see 4.2.1 for the cross-correlation metric results and 4.2.2 for the computation time results.

4.2.1 EDR extraction performance results

To implement cross-correlation evaluation metric, EDR signals and corresponding respiratory signals are stored considering the method, patient, and database. We then compute the cross-correlation between all EDR and respiratory signals from each patient to acquire the average for each method. This average then represents the overall performance of a particular method for the entirety of a patient's data. This procedure was performed for all subjects in each of databases in which the final mean cross-validation of each method was stored.

This information is shown for the Fantasia and Medical Radar databases in Fig. 4.5 and Fig. 4.6, respectively, these images represent a boxplot of the collected data, where the data is divided by their 4 quartiles. Here the interquartile range is represented by the colored areas and divided by the median of the data. The first quartile represents the data distribution below the interquartile range and the fourth quartile represents the data above it, while the outliers are represented as parallelograms. In Table. 4.2 for the Fantasia database and in Table. 4.3 for the Medical Radar database, the mean, median, standard deviation, and other descriptive elements of the cross-correlation of each method are shown. From this, we can see that all methods perform satisfactorily overall, with a mean cross-correlation above the 70% mark in both databases and most methods achieving a cross-correlation in the 80% range or even above.

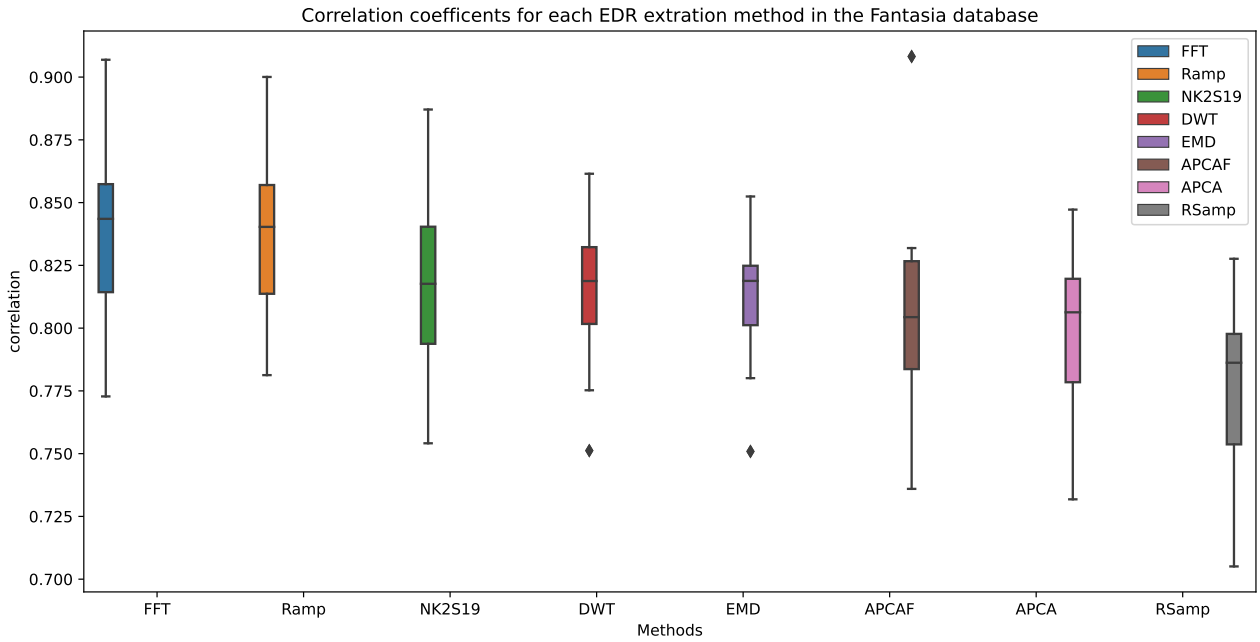

Figure 4.5: Cross-correlation for each EDR extraction method for each patient in the Fantasia database.The X-axis corresponds to methods of EDR extraction of the data and the Y-axis represent their cross-correlation score.Here the interquartile range is represented by the colored areas and divided by the median of the data. The first quartile represents the data distribution below the interquartile range and the fourth quartile represents the data above it, while the outliers are represented as parallelograms.

	FFT	**DWT**	**NK2S19**	**EMD**	**Ramp**	**RSamp**	**APCA**	**APCAF**
Number of subjects	29.0	29.0	29.0	29.0	29.0	29.0	29.0	29.0
mean	0.837	0.815	0.822	0.812	0.837	0.775	0.802	0.809
std	0.034	0.027	0.036	0.023	0.034	0.032	0.031	0.037
min	0.773	0.751	0.754	0.751	0.781	0.705	0.732	0.736
25%	0.814	0.801	0.794	0.801	0.814	0.754	0.778	0.784
50%	0.844	0.819	0.818	0.819	0.840	0.786	0.806	0.804
75%	0.857	0.832	0.840	0.825	0.857	0.798	0.820	0.827
max	0.907	0.862	0.887	0.852	0.900	0.828	0.847	0.908

Table 4.2: Description of the normalized cross-correlation for each EDR extraction method in the Fantasia database.

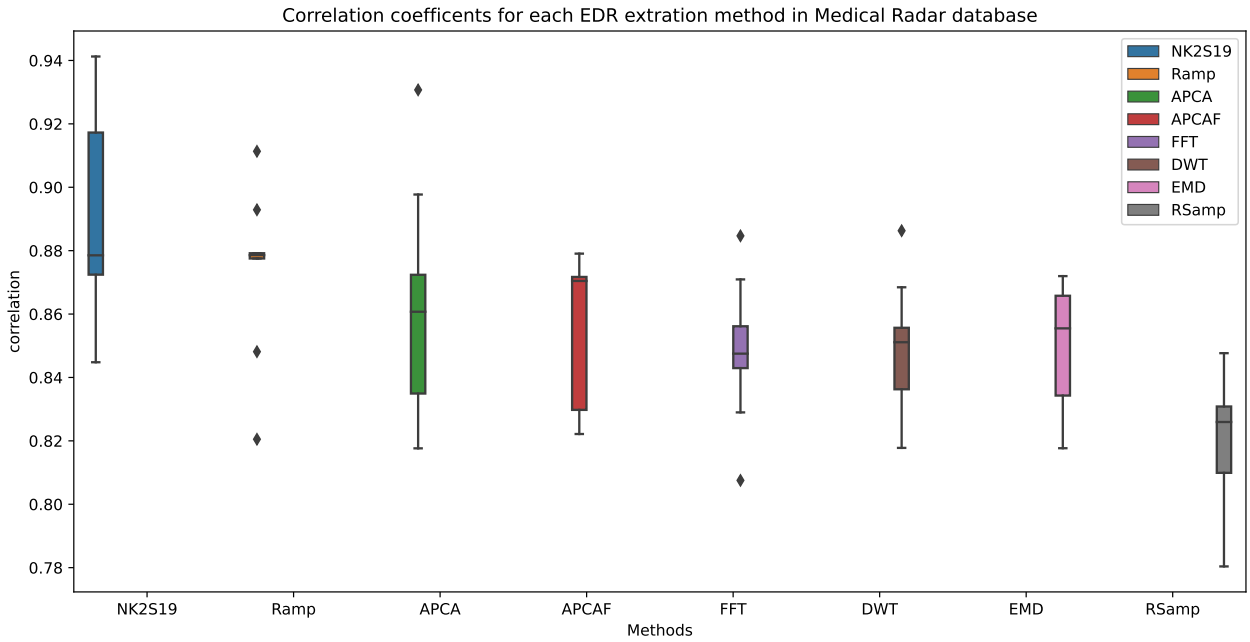

Figure 4.6: Cross-correlation for each EDR extraction method for each patient in the Medical Radar database. The X-axis corresponds to methods of EDR extraction of the data and the Y-axis represent their cross-correlation score.

	FFT	**DWT**	**NK2S19**	**EMD**	**Ramp**	**RSamp**	**APCA**	**APCAF**
Number of subjects	9.0	9.0	9.0	9.0	9.0	9.0	9.0	9.0
mean	0.848	0.848	0.889	0.847	0.874	0.818	0.862	0.857
std	0.022	0.021	0.030	0.021	0.026	0.022	0.036	0.024
min	0.808	0.818	0.844	0.818	0.820	0.780	0.818	0.822
25%	0.843	0.836	0.872	0.834	0.878	0.810	0.835	0.830
50%	0.848	0.851	0.879	0.855	0.879	0.826	0.861	0.870
75%	0.856	0.856	0.917	0.866	0.879	0.831	0.872	0.872
max	0.885	0.886	0.941	0.872	0.911	0.848	0.931	0.879

Table 4.3: Description of the normalized cross-correlation for each EDR extraction method in the Medical radar database.

Analyzing the result, we can also see that the FFT method is consistently close to the mean cross-correlation mark of 85% with narrower variance windows compared to other methods in both databases. As we can see in both Figures 4.2 and 4.3, this method tends to have most values in the upper part of its distribution. Although this algorithm is not the best performing algorithm in the Medical Radar database, it is still among the methods with the lowest variance of all methods tested in this database with performance above the

80 percent mark. This shows that the FFT method is an effective and overall robust method that can perform well in a variety of scenarios.

It can also be seen that the PCA methods are on par with the other methods with mean values around 80-81% in the Fantasia database and around 86% in the Medical Radar database. However, the performance of PCA methods compared to the other methods varies from database to database. In the Fantasia database, it is in the lower half of the tested methods, while in the Medical Radar database it is in the upper half. This difference in performance could be due to the incorrect detection of the R peaks, since the PCA algorithm is applied to the area around these peaks and therefore their correct detection can affect the PCA performance.

As for the performance differences between the results of the APCA and APCAF methods it can be neglected, since they perform very similarly in both databases. Nevertheless, the APCA method is preferable because it involves fewer steps and is therefore less computationally intensive. Overall, it can be concluded that the PCA methods can perform better than the reaming methods in certain scenarios.

The incorrect detection of R-peaks did not affect the R-peak methods as much, given that their overall performance when compared to the other methods did not change as much. Given that the Ramp method on the Medical Radar database with its high corss-correlation scored and very low variance could arguable be classified among the top three methods applied to that database, while still being in the second half of best performing methods for the Fantasia database. This could be due to the nature of the implemented R-peaks models, as they extract an EDR wave based on the relative amplitude distance between a reference point, the baseline in the ramp, and the R and S peaks in the RSamp. This means that the shape of the EDR signal is not greatly affected if the detected R-peaks differ slightly from the true ones, since these misdetections usually account for only a few points and thus the overall shape of the wave is preserved.

This is evident when analyzing the results of the Ramp, which reached a cross-correlation of about 83% in the Fantasia database and 87% in the Medical Radar database. In comparison, the mean cross-correlation of the RSamp method was 0.775% in the Fantasia database and 0.818% in the Medical Radar database. This shows not only that these methods are capable of achieving high values for cross-correlation, but also that the occasional misdetection of the QRS peaks, while not having a strong negative impact, can still reduce the performance of the methods. This reduction in performance is evident in the lower performance of the RSamp method compared to the Ramp method. This is most likely due to the fact that the RSamp method must accurately detect two peaks, and misdetection of even one of these peaks can negatively affect the EDR waveform and thus reduce performance. Which

resulted in the RSamp method being consistently the worst performing method.

The DWT approach behaved very similarly to the FFT method, achieving an average cross-correlation of 81 % in the Fantasia database and 84 % in the Medical Radar database. With the second lowest variance of all methods in the Medical Radar database. Where this difference in performance between the databases could be due to the fact that the selected parent wavelet was more similar to the breathing waves in the Medical Radar database than in the Fantasia database. This supports the idea that the correct choice of wavelet can significantly affect the results of the DWT.

The NK2S19s approach, originally used for comparison with other methods, proved to be one of the superior methods, especially in the Medical Radar database, where it achieved the highest score of all methods with a mean cross-correlation of 88%. As for the Fantasia database, although it was not the best method, it still achieved a cross-correlation of about 82%. This method also has the added advantage of being integrated into a Python library, requiring no prior knowledge of an EDR extraction algorithm or strategy, and providing the R-peak detection algorithm implemented in this study. Overall, this not only proves that this particular method can produce EDR signals that are very similar to the original respiratory signal, but also that with the exception of the RSamp method, the implemented algorithms perform similarly well, if not better, with this state-of-the-art approach.

As for the EMD method, it proved to be a very solid approach, as it was neither the best nor the worst under the circumstances tested. It is a robust method that has one of the lowest variances of all methods in all databases, with mean cross-correlation consistently above 80%. This makes it a stable algorithm that is perfectly suited for real-world applications and guarantees relatively high performance in a consistent manner. Thus, it is a method that can be used in any system as a fallback solution in case the other, better performing algorithms either fail or are not suitable for a particular scenario.

4.2.2 EDR extraction: time performance

The second evaluation metric implemented was the computation time for each method. These results can be seen in Figures 4.7 and 4.9 and in Figures 4.8 and 4.10. Starting with figures 4.7 and 4.9, they represent the average computation time that each method took to filter and extract an EDR in a single 30-second window, whose data analysis can be seen in Tables. 4.4 and 4.6. The figures 4.8 and 4.10 represent the average time required for a given method to analyze a patient's data from start to finish, whose data analysis can be seen in Tables. 4.5 and 4.7.

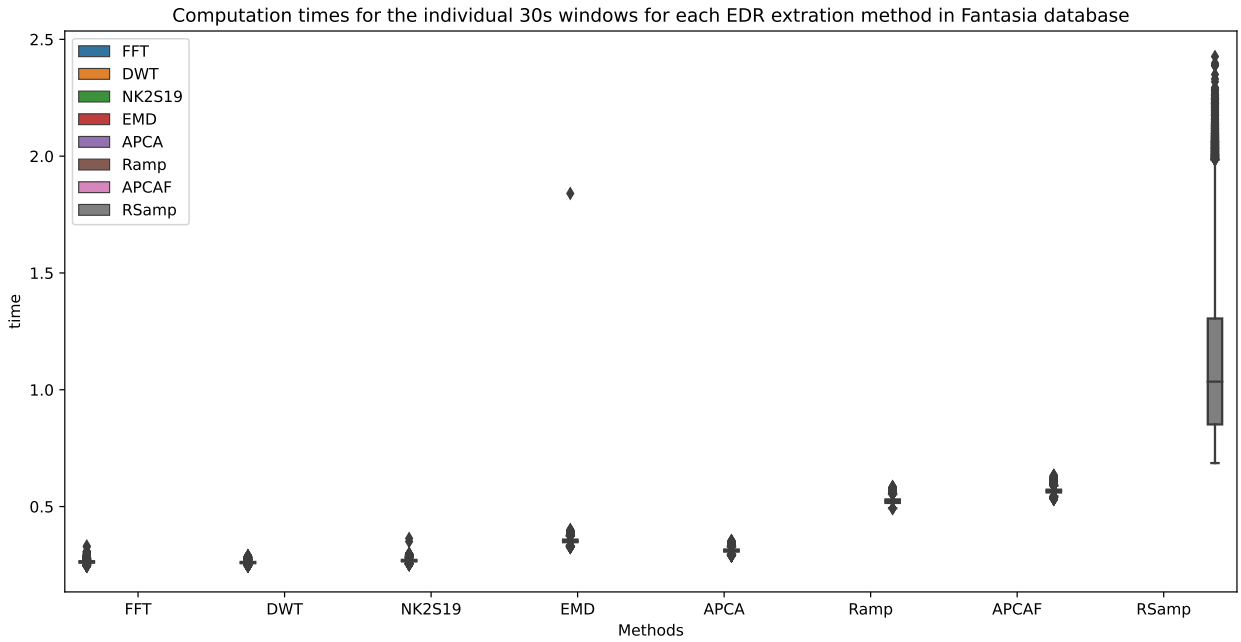

Figure 4.7: Computation time of each 30s window for each EDR extraction method in the Fantasia database. The X-axis corresponds to methods of EDR extraction of the data and the Y-axis represent their execution time in seconds.

	FFT	**DWT**	**NK2S19**	**EMD**	**Ramp**	**RSamp**	**APCA**	**APPCAF**
Number of subjects	106136.0	106136.0	106136.0	106136.0	106136.0	106136.0	106136.0	106136.0
mean	0.262	0.260	0.268	0.353	0.523	1.141	0.311	0.566
std	0.005	0.004	0.005	0.009	0.010	0.348	0.007	0.009
min	0.243	0.244	0.250	0.324	0.492	0.686	0.289	0.530
25%	0.260	0.257	0.265	0.347	0.516	0.852	0.307	0.560
50%	0.262	0.260	0.268	0.351	0.523	1.034	0.312	0.567
75%	0.266	0.263	0.272	0.359	0.531	1.305	0.316	0.572
max	0.331	0.290	0.364	1.840	0.586	2.426	0.354	0.634

Table 4.4: Description of the computation time for individual 30s windows for each method on the Fantasia database.

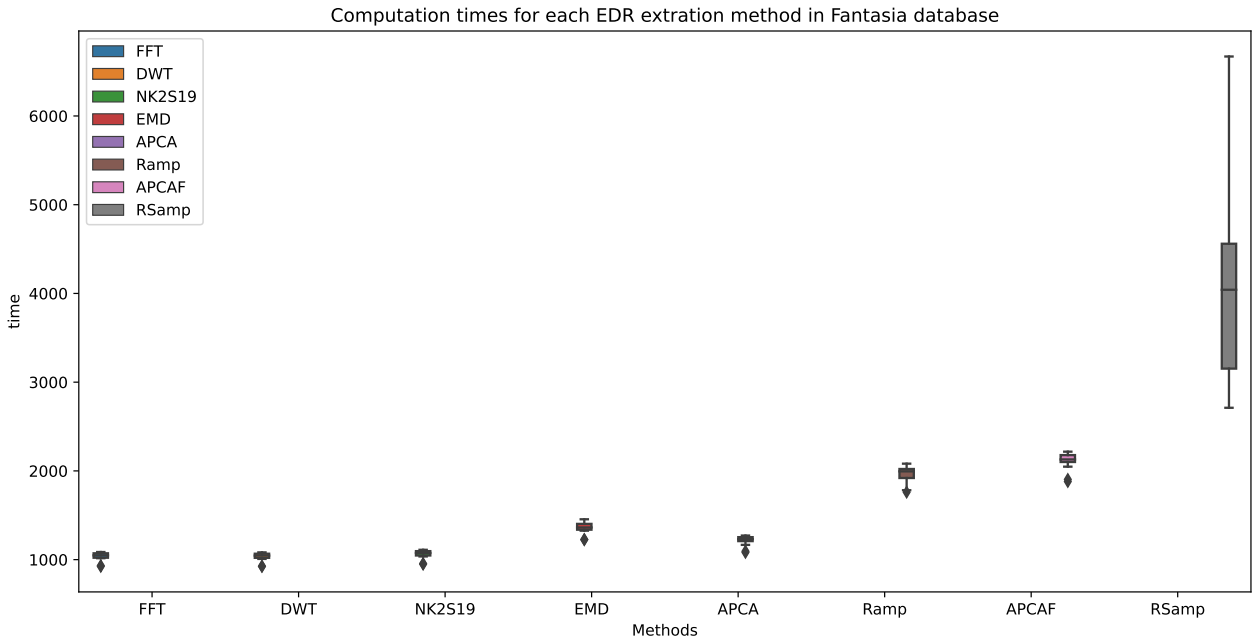

Figure 4.8: Computation time for each EDR extraction method in the Fantasia database. The X-axis corresponds to methods of EDR extraction of the data and the Y-axis represent their execution time in seconds.

	FFT	**DWT**	**NK2S19**	**EMD**	**Ramp**	**RSamp**	**APCA**	**APCAF**
Number of subjects	29.0	29.0	29.0	29.0	29.0	29.0	29.0	29.0
mean	1041.740	1037.836	1066.937	1367.061	1969.201	4099.882	1219.589	2121.473
std	39.639	39.261	40.653	53.762	76.117	1067.469	45.486	78.773
min	924.208	923.526	948.998	1224.420	1760.237	2711.368	1081.368	1880.022
25%	1021.500	1020.422	1046.862	1337.405	1919.976	3152.753	1208.586	2100.402
50%	1048.168	1045.771	1075.432	1362.528	1994.830	4041.264	1230.618	2129.160
75%	1071.503	1066.738	1095.830	1402.997	2021.520	4560.077	1253.447	2178.169
max	1085.855	1081.794	1110.890	1454.781	2081.575	6670.235	1271.413	2216.770

Table 4.5: Description of the computation time for each method on the Fantasia database.

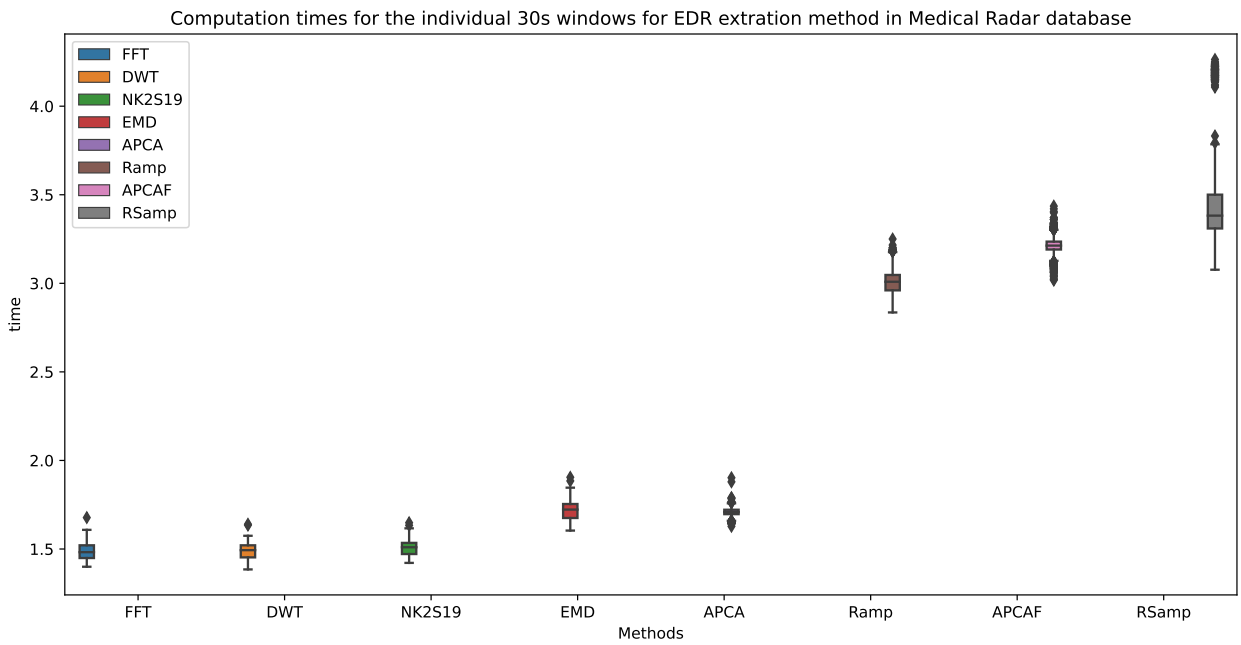

Figure 4.9: Computation time of each 30s window for each EDR extraction method in the Medical radar database. The X-axis corresponds to methods of EDR extraction of the data and the Y-axis represent their execution time in seconds.

	FFT	**DWT**	**NK2S19**	**EMD**	**Ramp**	**RSamp**	**APCA**	**APCAF**
Number of subjects	1213.0	1213.0	1213.0	1213.0	1213.0	1213.0	1213.0	1213.0
mean	1.486	1.487	1.506	1.720	3.010	3.469	1.707	3.213
std	0.045	0.040	0.040	0.052	0.078	0.291	0.023	0.054
min	1.400	1.384	1.422	1.604	2.836	3.077	1.628	3.018
25%	1.449	1.453	1.472	1.675	2.960	3.309	1.697	3.191
50%	1.482	1.494	1.510	1.722	3.009	3.382	1.708	3.212
75%	1.521	1.521	1.534	1.754	3.047	3.501	1.721	3.235
max	1.677	1.639	1.648	1.905	3.250	4.264	1.902	3.436

Table 4.6: Description of the computation time for each method on the Medical Radar database.

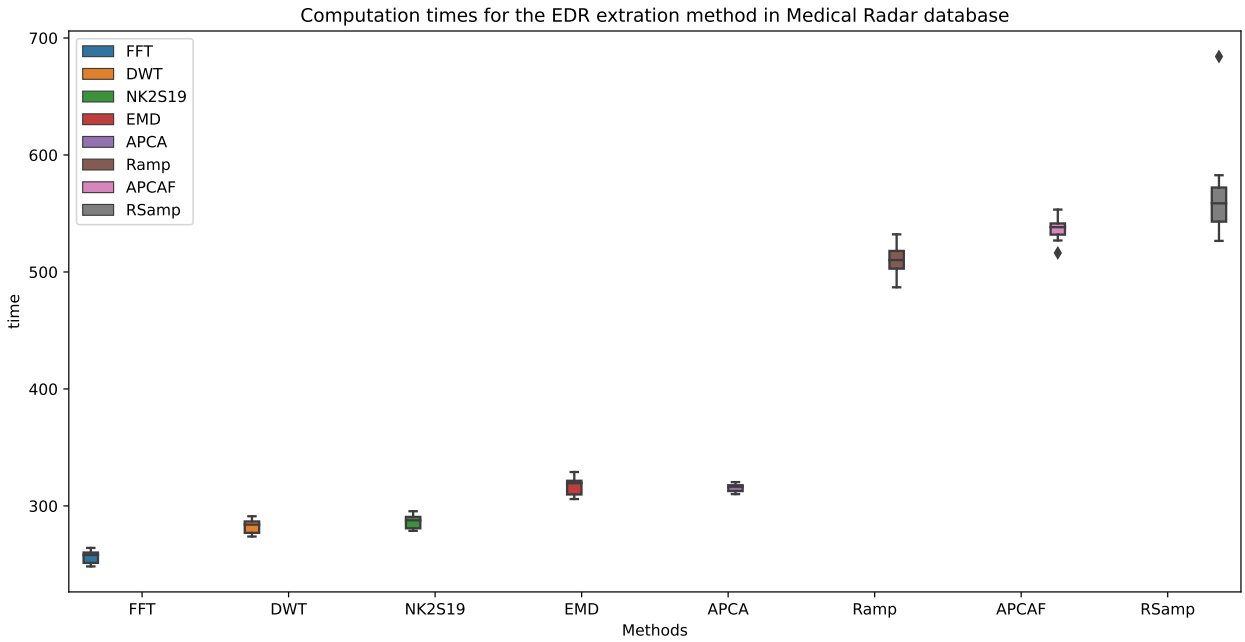

Figure 4.10: Description of the computation time for individual 30s windows for each method on the Medical radar database. The X-axis corresponds to methods of EDR extraction of the data and the Y-axis represent their execution time in seconds.

	FFT	**DWT**	**NK2S19**	**EMD**	**Ramp**	**RSamp**	**APCA**	**APCAF**
Number of subjects	9	9	9	9	9	9	9	9
mean	255.926	282.172	286.313	316.531	510.563	571.120	315.400	536.635
std	5.518	5.980	5.873	7.786	13.750	48.899	3.648	10.982
min	248.294	273.850	278.695	305.903	486.907	526.574	310.106	516.293
25%	251.313	277.0215	280.965	309.807	505.0211	544.001	313.830	534.427
50%	256.065	282.466	286.674	317.364	511.896	560.164	315.791	538.333
75%	259.710	286.562	290.415	320.618	516.399	572.531	317.138	540.731
max	264.105	291.177	295.479	328.994	532.167	684.187	320.364	553.321

Table 4.7: Description of the computation time for each method on the Medical Radar database.

From these figures we can see that the methods based on the extraction of R peaks, including the methods where the extraction of these peaks is only the first step, namely the PCA methods, tend to take more time. This is especially true for the RSamp method, since it not only requires interpolation to generate an EDR wave, but also needs to detect two peaks in all QRS complexes present in a given time window. Therefore, the RSamp method is not only slower than the Ramp method, but also the slowest overall. As for the PCA approaches, the use of median filters in APCAF proved to be a disadvantage, as APCAF

was not only slower than APCA in every scenario, but also among the slowest methods with Ramp and RSamp. It is also worth noting that while the time difference between APCA and the FFT, DWT, NK2S19 and EMD methods is not very large, the remaining methods are significantly slower.

As for the FFT, the DWT, NK2S19 , and EMD methods all proved to be equally fast, with the FFT being in the same range in terms of computation time. These methods had an average execution time in each 30-second window of less than half a second in the Fantasia database and proved to be the most suitable methods for use in a real-time scenario, since the sampling frequency of about 250 Hz or below is the most common frequency when this type of ECG is used.

As for the reliability of the methods for analyzing the QRS complex for a real-time system. One can conclude that they are not suitable for this type of implementation. This is because, although they are still faster than one second in the Fantasia database, they have a longer execution time compared to the other methods. This can lead to a non-negligible delay in a program that has to juggle multiple algorithms simultaneously in a real-time environment.

Thus, these results show that the FFT, DWT, NK2S19 , and EMD methods are interchangeable in terms of computation time and are best suited for real-time systems, although the FFT method is faster.

Finally, a comment on the times for the Medical Radar database: the average time for the 30-second window was significantly slower than for the Fantasia database for all methods, as was to be expected with such a data dense database. All of this is then reflected in the total time it took each method, on average, to fully analyze each patient. However, the results show that while the time required to analyze each 30-second window for a given method in the Fantasia database was much faster than the data in the Medical Radar database, the number of samples and the length of the Fantasia database meant that the latter required the longest analysis time.

In summary, given the overall results of the tested methods in terms of cross-correlation values and computation time, the FFT, DWT, NK2S19 and EMD are the best performing methods. Where the methods based on the analysis of the QRS complex were not only found to be less consistent, but were also generally much slower. With the best algorithm for analyzing the QRS complex being the APCA method, as it not only performed the best in cross-correlation, but also had the fastest times among them.

The reason why the FFT, DWT, NK2S19 and EMD algorithms are considered the best algorithms is because they achieve some of the highest values for cross-correlation or their value is very close to the values that are in the upper half. This means that even when other methods were occasionally able to take one of the top spots, the selected algorithms

were still above the threshold of 80% cross-correlation and thus provided consistently high scores. They were also among the most stable methods with some of the lowest variances of all methods tested, especially the EMD method. In addition, they all required virtually the same processing time, which was always less than half a second for a real-time system. This means that they are the fastest, most stable, and highest scoring methods in this study. However, since these methods have similar performance in both cross-correlation and computation time, and given their individual advantages in relation to each other, makes these methods, in the author opinion, interchangeable. This opinion is based on the fact that, given their similar performance, one method may be preferred over the other depending on which aspect is most important in a particular implementation. For a faster method, the FFT is the best option; the DWT is very similar to the FFT, but may be superior to it depending on the data and the mother wavelet. However, if the most important aspect is robustness, EMD is the best method.

This, and the fact that they outperformed or showed similar performance to a tested state-of-the-art method included in the NeuroKit2 Python library, proves that these methods can be used in real systems with relative robustness and performance. Thus, it was shown that the implemented methods can extract a respiratory signal from the ECG with considerable accuracy and therefore can be used in combination with other respiratory signals, allowing continuous monitoring of respiration even if one of the methods fails.

4.2.3 EDR extraction validation on the WoW project belt data

To further validate the EDR extraction algorithms implemented in this study, a subject was asked to wear the WoW project belt (see Fig. 4.1) to extract both ECG and respiratory data from the latest and most stable version of the belt to date. A dataset was created to employ the same methodology as with the databases. This was done not only to verify that the implemented EDR methods were robust enough to be used in the project, but also to test them in the same way as the databases and compare their results in more detail. Therefore, the same procedure as in section 4.2 was used in this section. However, it is worth noting that the ECG sensor (128 Hz) and the respiration sensor (10 Hz) had different sampling frequencies. Therefore, the respiration data was interpolated with cubic spline to treat them as if they were acquired at the same sampling frequency as the ECG.

As we can see in Fig. 4.11, the results are similar to those in 4.2. Although sony2019 showed lower performance than usual, both the FFT, DWT and EMD methods achieved high cross-correlation rates and were among the best evaluated methods. The APCA and APCAF methods, as mentioned earlier, performed very high scores of cross-correlation, and in this particular case even outperformed most of the methods by being about on par with

the second best method. Once again, the use of a median filter in APCAF proved to have no major impact in its of cross-correlation performance when compared to the APCA. Both the Ramp and RSamp algorithms performed similarly to the databases. Whereby the RSamp method performed inferiorly to Ramp in terms of cross-correlation.

These results also prove that the algorithms implemented in this study are general and robust enough to handle data from the WoW project belt and can be used in future research on a real-time system. This could be done by using these methods as a secondary signal to improve the quality of respiration monitoring or even as the main source of information for a respiration signal.

However, it should be noted that these values were measured in a very controlled manner when the project's belt was in a very stable configuration and fully operational, and the subject was in stable positions, such as standing, sitting, andlayingdown. Therefore, further studies should be conducted to improve the general conditions of the belt to be able to deal with more unstable positions.

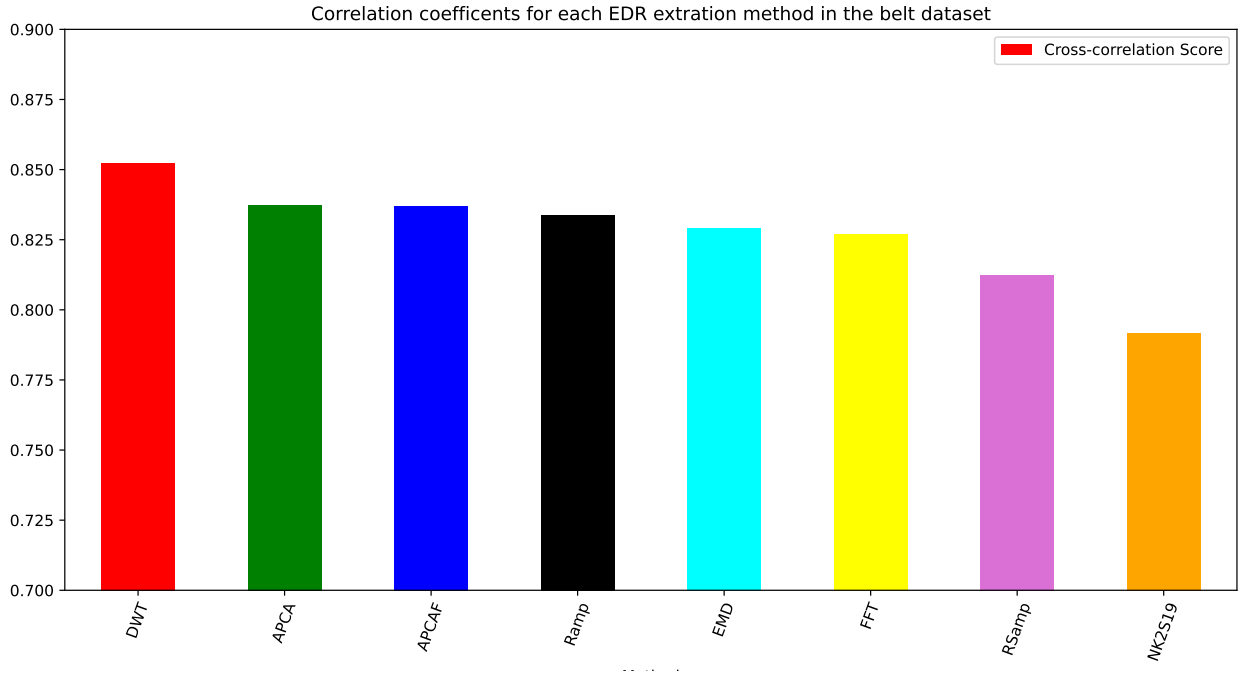

Figure 4.11: Mean cross-correlation values for the validation data of the WoW project belt. The X-axis corresponds to methods of EDR extraction of the data and the Y-axis represent their cross-correlation score.

5 Conclusion

This dissertation focuses on the application of automated algorithms to extract respiratory rate and EDR signals for continuous monitoring of patient breathing. We provide an overview of the current state of the art on the use of multiple sensors for healthcare. In doing so, we identified which signals currently being monitored in healthcare are central to monitoring a patient's well-being. Therefore, it was decided to prioritize respiratory monitoring, whereupon a respiratory rate extraction study was conducted. This study led to a better understanding of how the use of multiple sensors can benefit knowledge discovery algorithms. This includes increasing the robustness of the extracted data as well as the ability to extract the same data from different sensors. This is important because it demonstrates the ability to extract a repiration wave from the ECG signal. For this reason, a review of EDR extraction techniques was also conducted. From this, a selection was made of the best tested and best performing methods that were most suitable for the real-time applications and limited resources of this dissertation. In addition, a state-of-the-art method from the NeuroKit2 library was included to allow a more direct comparison of the implemented models with the current state of the art in EDR extraction.

To determine the respiration rate from a respiration wave, an algorithm was implemented that focused on detecting individual respiration cycles, i.e., each set of one minimum and two maxima present in a respiration wave. This particular algorithm proved capable of running in real time.

The algorithm implemented a 3-window strategy of 5, 8, and 15 seconds each, running continuously on a 30-second buffer of filtered data. This was done to have specific windows for more accurate classification of breathing depending on whether a patient was breathing rapidly, normally, or slowly. This approach proved efficient, as counting of respiration rate showed that the system could accurately classify the current respiration rate in most cases

However, due to the physical structure of the belt, the respiratory sensor, and the algorithm, performance was lower when the subject was in an unstable position, such as walking or running. To combat these issues and provide an auxiliary system to monitor a patient's breathing, several approaches were implemented that focused on using the ECG sensor to

extract a respiratory wave, i.e., EDR. This was done not only to have a second source of respiratory monitoring, but also to test whether these approaches were robust enough to replace the respiratory sensor.

The original plan was to also test these approaches with the belt's data in real time, but unfortunately this was not possible during this transition phase because the project belt's hardware suffered from instability. It was not uncommon for the belt to fail during use, making it almost impossible to re-establish the connection within a short period of time. In addition, there were also problems with the physical structure of the sensors. These problems often led to a physical interruption of the connection between the sensors or to electrical disturbances that distorted the signal to such an extent that it was sometimes impossible to recognize the measured phenomenon in the recorded signals. This led to numerous changes in the hardware and firmware of the various components that made up the belt, as well as some changes in the materials of the sensors themselves to increase their durability and overall precision.

Nevertheless, it was possible to perform a very controlled test with the latest and most robust version of the project belt, where the tested EDR extraction algorithms were able to achieve a high degree of cross-correlation between the extracted EDR signals and the respiratory signal. However, the obtained results suggest that EDR methods could potentially replace the respiratory sensor. However, since they are sometimes unable to detect more unusual waveforms, they should rather be used as a secondary source for monitoring respiration. Namely, as a confirmatory source that is either merged with the original respiratory signal, or as a secondary signal to which the respiratory rate calculation is also applied and used for comparison with that calculated from the respiratory wave, or as a source when the respiratory sensor is not available.

Unfortunately, these methods have not yet been tested in a real-time scenario in a less controlled environment, since the performance of the belt, while improved, is not yet sufficient for a real-time test. This is because the data collected during validation requires that the belt be held in place by an external force to prevent it from moving or stretching, limiting the activities that a subject can perform. Therefor it is not possible to conclude the impact that more unstable positions such as walking can have in the performance of the EDR extraction algorithms, for which further studies must be conducted..

Given these circumstances, it was decided to test the EDR extraction techniques on separate, commonly available databases. This was done not only to further the development of the EDR algorithms, but also to compare the tested algorithms with other techniques. However it is important to highlight that there was no positional information associated with the databases chosen therefor it is was not possible to verfy the EDR algorithms robustness

for any given posture or activity.

The result of the tests performed with the EDR algorithms in the databases shows that these methods are not only comparable to the current state of the art, but even surpass it in some scenarios. This proves that the currently implemented methods are able to perform satisfactorily with respect to the current paradigm of EDR extraction, while being robust enough to perform adequately in different scenarios in widely used databases. Their final results are also very similar to the results observed for the belt data.

Another open issue is that no comparison of the performance of the respiratory rate algorithm proposed in this dissertation between the extracted EDR waves and the original respiratory rate waves has been performed, nor the percentage error between the calculated respiratory rate and the respiratory rate manually counted by a professional, which could be investigated in a future study. Another possible study could examine the fusion of EDR and respiratory wave to see if this fusion eliminates some of the noise. Where, the respiratory rate algorithm could also be implemented for both the original respiratory rate, the EDR waves, and the wave resulting from the fusion.

It is also worth noting that another approach, in which the patient's respiratory rate is derived directly from the ECG rather than the respiratory wave, using ML algorithms, particularly deep neural networks, has also been tested. In this approach, a variety of methods were tested, from Resnets, CNN-LSTM, LSTM, pure deep neural networks, autoencoders, as well as a number of combinations of these techniques, hyperparameters, and input signals.

However, the best model tested to date, CNN-LSTM, suffered from overfitting, as its validation and test accuracy was around 60-65%, but never above 70%. It was not considered competitive with the other implemented methods and thus was not mentioned as it remains open for future research.

Although there are still unresolved issues, this study demonstrated the potential of using multiple sensors for knowledge extraction, especially with respect to respiratory signals. It paved the way for implementing the present algorithms on a real-time system for future research. In which other algorithms that could use the implemented methods as a basis or as a secondary or primary source for increased robustness of measurements and knowledge extraction.

6 Bibliography

[1] D1.2: Functional specification and system integration architecture © 2020 all rights reserved. this document may not be reproduced in whole or in part, by photo- copy or other means, without the permission of the consortium. 2020.

[2] Qrs complex, Sep 2022. URL `https://en.wikipedia.org/wiki/QRS_complex#/media/File:SinusRhythmLabels.svg`.

[3] A. U. Alahakone and S. A. Senanayake. A real-time system with assistive feedback for postural control in rehabilitation. *IEEE/ASME Transactions on Mechatronics*, 15(2): 226–233, 2010.

[4] F. Azuaje, W. Dubitzky, N. Black, and K. Adamson. Improving clinical decision support through case-based data fusion. *IEEE Transactions on biomedical engineering*, 46(10): 1181–1185, 1999.

[5] S. Beck, B. Laufer, S. Krueger-Ziolek, and K. Moeller. Measurement of respiratory rate with inertial measurement units. *Current Directions in Biomedical Engineering*, 6(3): 237–240, 2020.

[6] E. Blasch, A. Steinberg, S. Das, J. Llinas, C. Chong, O. Kessler, E. Waltz, and F. White. Revisiting the jdl model for information exploitation. In *Proceedings of the 16th International Conference on Information Fusion*, pages 129–136. IEEE, 2013.

[7] J. Boyle, N. Bidargaddi, A. Sarela, and M. Karunanithi. Automatic detection of respiration rate from ambulatory single-lead ecg. *IEEE Transactions on Information Technology in Biomedicine*, 13(6):890–896, 2009.

[8] I. Brown. Modelling future landscape change on coastal floodplains using a rule-based gis. *Environmental Modelling & Software*, 21(10):1479–1490, 2006.

[9] M. Burrows, N. Eckhaus, D. Grube, and G. Christoffersen. Medication adherence system for and method of monitoring a patient medication adherence and facilitating dose reminders, Feb. 20 2014. US Patent App. 14/042,768.

[10] F. Castells, P. Laguna, L. Sörnmo, A. Bollmann, and J. M. Roig. Principal component analysis in ecg signal processing. *EURASIP Journal on Advances in Signal Processing*, 2007:1–21, 2007.

[11] A. Cesareo, Y. Previtali, E. Biffi, and A. Aliverti. Assessment of breathing parameters using an inertial measurement unit (imu)-based system. *Sensors*, 19(1):88, 2019.

[12] P. H. Charlton, D. A. Birrenkott, T. Bonnici, M. A. Pimentel, A. E. Johnson, J. Alastruey, L. Tarassenko, P. J. Watkinson, R. Beale, and D. A. Clifton. Breathing rate estimation from the electrocardiogram and photoplethysmogram: A review. *IEEE reviews in biomedical engineering*, 11:2–20, 2017.

[13] K. Edanami and G. Sun. Medical radar signal dataset for non-contact respiration and heart rate measurement. *Data in brief*, 40:107724, 2022.

[14] F. Famá, J. N. Faria, and D. Portugal. An iot-based interoperable architecture for wireless biomonitoring of patients with sensor patches. *Internet of Things*, 19:100547, 2022.

[15] F. Felisberto, A. Pereira, et al. A ubiquitous and low-cost solution for movement monitoring and accident detection based on sensor fusion. *Sensors*, 14(5):8961–8983, 2014.

[16] F. Felisberto, A. Pereira, et al. A ubiquitous and low-cost solution for movement monitoring and accident detection based on sensor fusion. *Sensors*, 14(5):8961–8983, 2014.

[17] G. Fleming, M. Van der Merwe, and G. McFerren. Fuzzy expert systems and gis for cholera health risk prediction in southern africa. *Environmental Modelling & Software*, 22(4):442–448, 2007.

[18] G. Fortino and R. Gravina. Fall-mobileguard: A smart real-time fall detection system. In *Proceedings of the 10th EAI International Conference on Body Area Networks*, pages 44–50, 2015.

[19] G. Fortino, D. Parisi, V. Pirrone, and G. Di Fatta. Bodycloud: A saas approach for community body sensor networks. *Future Generation Computer Systems*, 35:62–79, 2014.

[20] L. Gao, A. K. Bourke, and J. Nelson. Activity recognition using dynamic multiple sensor fusion in body sensor networks. In *2012 Annual International Conference of the IEEE Engineering in Medicine and Biology Society*, pages 1077–1080. IEEE, 2012.

[21] D. Geeta, N. Nalini, and R. C. Biradar. Fault tolerance in wireless sensor network using hand-off and dynamic power adjustment approach. *Journal of Network and Computer Applications*, 36(4):1174–1185, 2013.

[22] H. Ghasemzadeh, P. Panuccio, S. Trovato, G. Fortino, and R. Jafari. Power-aware activity monitoring using distributed wearable sensors. *IEEE Transactions on Human-Machine Systems*, 44(4):537–544, 2014.

[23] H. Ghasemzadeh, P. Panuccio, S. Trovato, G. Fortino, and R. Jafari. Power-aware activity monitoring using distributed wearable sensors. *IEEE Transactions on Human-Machine Systems*, 44(4):537–544, 2014.

[24] A. L. Goldberger, L. A. Amaral, L. Glass, J. M. Hausdorff, P. C. Ivanov, R. G. Mark, J. E. Mietus, G. B. Moody, C.-K. Peng, and H. E. Stanley. Physiobank, physiotoolkit, and physionet: components of a new research resource for complex physiologic signals. *circulation*, 101(23):e215–e220, 2000.

[25] R. Gravina, P. Alinia, H. Ghasemzadeh, and G. Fortino. Multi-sensor fusion in body sensor networks: State-of-the-art and research challenges. *Information Fusion*, 35:68–80, 2017.

[26] S. Härtel, J.-P. Gnam, S. Löffler, and K. Bös. Estimation of energy expenditure using accelerometers and activity-based energy models—validation of a new device. *European Review of Aging and Physical Activity*, 8(2):109–114, 2011.

[27] M. K. Hasan, H. A. Rubaiyeat, Y.-K. Lee, and S. Lee. A reconfigurable hmm for activity recognition. In *2008 10th International Conference on Advanced Communication Technology*, volume 1, pages 843–846. IEEE, 2008.

[28] J. He, H. Li, and J. Tan. Real-time daily activity classification with wireless sensor networks using hidden markov model. In *2007 29th Annual international conference of the IEEE engineering in medicine and biology society*, pages 3192–3195. IEEE, 2007.

[29] E. Helfenbein, R. Firoozabadi, S. Chien, E. Carlson, and S. Babaeizadeh. Development of three methods for extracting respiration from the surface ecg: a review. *Journal of electrocardiology*, 47(6):819–825, 2014.

[30] P. Hung, S. Bonnet, R. Guillemaud, E. Castelli, and P. T. N. Yen. Estimation of respiratory waveform using an accelerometer. In *2008 5th IEEE International symposium on biomedical imaging: from nano to macro*, pages 1493–1496. IEEE, 2008.

[31] P. Janbakhshi and M. B. Shamsollahi. Ecg-derived respiration estimation from single-lead ecg using gaussian process and phase space reconstruction methods. *Biomedical Signal Processing and Control*, 45:80–90, 2018.

[32] Y. Jiang and L. Chongwu. Design and test of high precision relative thermometer. In *2013 Fifth International Conference on Measuring Technology and Mechatronics Automation*, pages 431–433. IEEE, 2013.

[33] E. Kalapanidas and N. Avouris. Short-term air quality prediction using a case-based classifier. *Environmental Modelling & Software*, 16(3):263–272, 2001.

[34] I. Keramitsoglou, C. Cartalis, and C. T. Kiranoudis. Automatic identification of oil spills on satellite images. *Environmental modelling & software*, 21(5):640–652, 2006.

[35] K. C. A. Khanzode and R. D. Sarode. Advantages and disadvantages of artificial intelligence and machine learning: A literature review. *International Journal of Library & Information Science (IJLIS)*, 9(1):3, 2020.

[36] J. Kim, J. Hong, N. Kim, E. Cha, and T.-S. Lee. Two algorithms for detecting respiratory rate from ecg signal. In *World Congress on Medical Physics and Biomedical Engineering 2006*, pages 4069–4071. Springer, 2007.

[37] P. Langley, E. J. Bowers, and A. Murray. Principal component analysis as a tool for analyzing beat-to-beat changes in ecg features: application to ecg-derived respiration. *IEEE transactions on biomedical engineering*, 57(4):821–829, 2009.

[38] B. C. Lau, E. W. Ma, and T. W. Chow. Probabilistic fault detector for wireless sensor network. *Expert Systems with Applications*, 41(8):3703–3711, 2014.

[39] B.-H. Lee, M. Scholz, A. Horn, and A. M. Furber. Constructed wetlands: prediction of performance with case-based reasoning (part b). *Environmental engineering science*, 23(2):332–340, 2006.

[40] G. Lee, R. Gommers, F. Waselewski, K. Wohlfahrt, and A. O'Leary. Pywavelets: A python package for wavelet analysis. *Journal of Open Source Software*, 4(36):1237, 2019.

[41] H. Lim, B. Kim, and S. Park. Prediction of lower limb kinetics and kinematics during walking by a single imu on the lower back using machine learning. *Sensors*, 20(1):130, 2020.

[42] P. Lopez-Meyer and E. Sazonov. Automatic breathing segmentation from wearable respiration sensors. In *2011 Fifth International Conference on Sensing Technology*, pages 156–160. IEEE, 2011.

[43] Y. Lu, M. Wang, W. Wu, Y. Han, Q. Zhang, and S. Chen. Dynamic entropy-based pattern learning to identify emotions from eeg signals across individuals. *Measurement*, 150:107003, 2020.

[44] R. C. Luo, C.-C. Yih, and K. L. Su. Multisensor fusion and integration: approaches, applications, and future research directions. *IEEE Sensors journal*, 2(2):107–119, 2002.

[45] K. V. Madhav, M. R. Ram, E. H. Krishna, N. R. Komalla, and K. A. Reddy. Estimation of respiration rate from ecg, bp and ppg signals using empirical mode decomposition. In *2011 IEEE International Instrumentation and Measurement Technology Conference*, pages 1–4. IEEE, 2011.

[46] D. Makowski, T. Pham, Z. J. Lau, J. C. Brammer, F. Lespinasse, H. Pham, C. Schölzel, and S. H. A. Chen. NeuroKit2: A python toolbox for neurophysiological signal processing. *Behavior Research Methods*, 53(4):1689–1696, feb 2021. doi: 10.3758/s13428-020-01516-y. URL `https://doi.org/10.3758%2Fs13428-020-01516-y`.

[47] T. Martin, B. Majeed, B.-S. Lee, and N. Clarke. Fuzzy ambient intelligence for next generation telecare. In *2006 IEEE International Conference on Fuzzy Systems*, pages 894–901. IEEE, 2006.

[48] L. Mo, S. Liu, R. X. Gao, and P. S. Freedson. Energy-efficient and data synchronized body sensor network for physical activity measurement. In *2013 IEEE International Instrumentation and Measurement Technology Conference (I2MTC)*, pages 1120–1124. IEEE, 2013.

[49] M. Nazari and S. M. Sakhaei. Variational mode extraction: A new efficient method to derive respiratory signals from ecg. *IEEE journal of biomedical and health informatics*, 22(4):1059–1067, 2017.

[50] C. Orphanidou. Derivation of respiration rate from ambulatory ecg and ppg using ensemble empirical mode decomposition: Comparison and fusion. *Computers in biology and medicine*, 81:45–54, 2017.

[51] S.-B. Park, Y.-S. Noh, S.-J. Park, and H.-R. Yoon. An improved algorithm for respiration signal extraction from electrocardiogram measured by conductive textile electrodes using instantaneous frequency estimation. *Medical & biological engineering & computing*, 46(2):147–158, 2008.

[52] A. J. Quinn, V. Lopes-dos Santos, D. Dupret, A. C. Nobre, and M. W. Woolrich. Emd: Empirical mode decomposition and hilbert-huang spectral analyses in python.

Journal of Open Source Software, 6(59):2977, 2021. doi: 10.21105/joss.02977. URL https://doi.org/10.21105/joss.02977.

[53] M. Rahman and B. I. Morshed. Estimation of respiration rate using an inertial measurement unit placed on thorax-abdomen. In *2021 IEEE International Conference on Electro Information Technology (EIT)*, pages 1–5. IEEE, 2021.

[54] A. Ramesh, C. Kambhampati, J. R. Monson, and P. Drew. Artificial intelligence in medicine. *Annals of the Royal College of Surgeons of England*, 86(5):334, 2004.

[55] A. K. Raz, C. R. Kenley, and D. A. DeLaurentis. A system-of-systems perspective for information fusion system design and evaluation. *Information Fusion*, 35:148–165, 2017.

[56] L. C. Rodrigues and M. Marengoni. Detecting qrs complex in ecg using wavelets and cubic spline interpolation. *Biomedical Engineering*, 9(1), 2012.

[57] R. Ruangsuwana, G. Velikic, and M. Bocko. Methods to extract respiration information from ecg signals. In *2010 IEEE International Conference on Acoustics, Speech and Signal Processing*, pages 570–573. IEEE, 2010.

[58] M. Ryan. Decomposing signal using empirical mode decomposition-algorithm explanation for dummy, Nov 2019. URL https://towardsdatascience.com/decomposing-signal-using-empirical-mode-decomposition-algorithm-explanation-for-d

[59] N. Sadr and P. de Chazal. A fast approximation method for principal component analysis applied to ecg derived respiration for osa detection. In *2016 38th Annual International Conference of the IEEE Engineering in Medicine and Biology Society (EMBC)*, pages 6198–6201. IEEE, 2016.

[60] H. Sampathkumar, X.-w. Chen, and B. Luo. Mining adverse drug reactions from online healthcare forums using hidden markov model. *BMC medical informatics and decision making*, 14(1):1–18, 2014.

[61] F. Sanfilippo and K. Y. Pettersen. A sensor fusion wearable health-monitoring system with haptic feedback. In *2015 11th International conference on innovations in information technology (IIT)*, pages 262–266. IEEE, 2015.

[62] A. E. E. Santo and C. Carbajal. Respiration rate extraction from ecg signal via discrete wavelet transform. In *2010 2nd Circuits and Systems for Medical and Environmental Applications Workshop (CASME)*, pages 1–4. IEEE, 2010.

[63] A. E. E. Santo and C. Carbajal. Respiration rate extraction from ecg signal via discrete wavelet transform. In *2010 2nd Circuits and Systems for Medical and Environmental Applications Workshop (CASME)*, pages 1–4. IEEE, 2010.

[64] H. Sedghamiz. Biosigkit: a matlab toolbox and interface for analysis of biosignals. *Journal of Open Source Software*, 3(30):671, 2018.

[65] H. Sharma, K. Sharma, and O. L. Bhagat. Respiratory rate extraction from single-lead ecg using homomorphic filtering. *Computers in biology and medicine*, 59:80–86, 2015.

[66] F. Shi, J. Wang, J. Shi, Z. Wu, Q. Wang, Z. Tang, K. He, Y. Shi, and D. Shen. Review of artificial intelligence techniques in imaging data acquisition, segmentation, and diagnosis for covid-19. *IEEE reviews in biomedical engineering*, 14:4–15, 2020.

[67] A. Sobron, I. Romero, and T. Lopetegi. Evaluation of methods for estimation of respiratory frequency from the ecg. In *2010 Computing in Cardiology*, pages 513–516. IEEE, 2010.

[68] B. Spetzler, J. Su, R.-M. Friedrich, F. Niekiel, S. Fichtner, F. Lofink, and F. Faupel. Influence of the piezoelectric material on the signal and noise of magnetoelectric magnetic field sensors based on the delta-e effect. *APL Materials*, 9(3):031108, 2021.

[69] K. T. Sweeney, D. Kearney, T. E. Ward, S. Coyle, and D. Diamond. Employing ensemble empirical mode decomposition for artifact removal: extracting accurate respiration rates from ecg data during ambulatory activity. In *2013 35th Annual International Conference of the IEEE Engineering in Medicine and Biology Society (EMBC)*, pages 977–980. IEEE, 2013.

[70] R. R. Tan. Rule-based life cycle impact assessment using modified rough set induction methodology. *Environmental modelling & software*, 20(5):509–513, 2005.

[71] E. Teitelbaum, K. W. Chen, F. Meggers, H. Guo, N. Houchois, J. Pantelic, and A. Rysanek. Globe thermometer free convection error potentials. *Scientific reports*, 10(1):1–13, 2020.

[72] M. Wainberg, D. Merico, A. Delong, and B. J. Frey. Deep learning in biomedicine. *Nature biotechnology*, 36(9):829–838, 2018.

[73] D. Widjaja, C. Varon, A. Dorado, J. A. Suykens, and S. Van Huffel. Application of kernel principal component analysis for single-lead-ecg-derived respiration. *IEEE Transactions on Biomedical Engineering*, 59(4):1169–1176, 2012.

[74] S.-H. Zahiri and S.-A. Seyedin. Swarm intelligence based classifiers. *Journal of the Franklin Institute*, 344(5):362–376, 2007.

[75] P. Zappi, T. Stiefmeier, E. Farella, D. Roggen, L. Benini, and G. Troster. Activity recognition from on-body sensors by classifier fusion: sensor scalability and robustness. In *2007 3rd international conference on intelligent sensors, sensor networks and information*, pages 281–286. IEEE, 2007.

[76] A. Zarei and B. M. Asl. Automatic classification of apnea and normal subjects using new features extracted from hrv and ecg-derived respiration signals. *Biomedical Signal Processing and Control*, 59:101927, 2020.

[77] H. Zhang, H. Li, and C. Tam. Particle swarm optimization for resource-constrained project scheduling. *International Journal of Project Management*, 24(1):83–92, 2006.